Narrow dip inside a natural linewidth absorption profile in a system of two atoms

A. A. Makarov*

Institute of Spectroscopy, Russian Academy of Sciences, 5 Fizicheskaya Street, Troitsk, Moscow 142190, Russia
and Moscow Institute of Physics and Technology, 9 Institutskiy Pereulok, Dolgoprudny, Moscow Region 141700, Russia

(Received 23 January 2015; published 17 November 2015)

Absorption spectrum of a system of two closely spaced identical atoms displays, at certain preparation, a dip that can be much narrower than the natural linewidth. This preparation includes (i) application of a strong magnetic field at an angle α, that is very close to the magic angle $\alpha_0 = \arccos(1/\sqrt{3}) \approx 54.7^\circ$, with respect to the direction from one atom to another, and (ii) in-plane illumination by a laser light in the form of a nonresonant standing wave polarized at the same angle α. Both qualitative and quantitative arguments for the narrow dip effect are presented.

DOI: 10.1103/PhysRevA.92.053840 PACS number(s): 42.50.Ct, 32.70.Jz

I. INTRODUCTION

One of the famous Fano's problems is called "A Number of Discrete States and One Continuum" [1]. Although the main subject of Ref. [1] is atomic autoionization states embedded into the ionization continuum, the method of solution is generic and can be applied to other systems, e.g., the "atom plus quantized electromagnetic field" [2]. So, let the Fano's one continuum states be direct products $|0\rangle\otimes|1_x^{(s)}\rangle$ of the ground atomic state $|0\rangle$ and the one-photon wave packet $|1_x^{(s)}\rangle$ of an arbitrary frequency x and a definite polarization s with respect to a fixed quantization axis of projection M of the atom angular momentum. Also, let the Fano's number of discrete states be two direct products $|1\rangle\otimes|\mathrm{vac}\rangle$, $|2\rangle\otimes|\mathrm{vac}\rangle$ of the excited atomic states $|1\rangle$, $|2\rangle$ and the vacuum state of the electromagnetic field. Then, if the both spontaneous transitions $|1\rangle \to |0\rangle$ and $|2\rangle \to |0\rangle$ are of the same polarization s and their frequencies ω_{10} and ω_{20} are *very close*, the Fano's solution leads to an intriguing result: the spectrum of linear absorption (in the framework of the Weisskopf-Wigner idealization [3]), being

$$\mathcal{A}(\omega) = \frac{1}{2\pi(\Gamma_1+\Gamma_2)} \times \frac{[\Gamma_1(\omega-\omega_{20})+\Gamma_2(\omega-\omega_{10})]^2}{(\omega-\omega_{10})^2(\omega-\omega_{20})^2+\frac{1}{4}[\Gamma_1(\omega-\omega_{20})+\Gamma_2(\omega-\omega_{10})]^2} \tag{1}$$

where Γ_1 and Γ_2 are spontaneous emission rates, can exhibit a narrow dip with zero absorption at the frequency of

$$\bar{\omega} = \frac{\Gamma_1\omega_{20}+\Gamma_2\omega_{10}}{\Gamma_1+\Gamma_2} \tag{2}$$

between ω_{10} and ω_{20}. The width (full width at half maximum) of this dip is equal to

$$\sigma = \sqrt{\tfrac{1}{4}(\Gamma_1+\Gamma_2)^2+(\omega_{20}-\omega_{10})^2} - \tfrac{1}{2}(\Gamma_1+\Gamma_2), \tag{3}$$

and it can be narrower than $(\Gamma_1+\Gamma_2)/2$. Several examples with $\Gamma_1 = \Gamma_2 = \Gamma$ are shown in Fig. 1. The effect is due to destructive interference of the probability amplitudes of states $|1\rangle$ and $|2\rangle$ in the exact continuous-spectrum eigenstates lying between ω_{10} and ω_{20}. (The same result including a picture like Fig. 1 was obtained in Ref. [4] using the density matrix formalism.)

It can be assumed that an observation of such narrow resonance structure (presumably controllable, in addition, by external fields) would attract some attention—the same as to a variety of other effects of quantum interference and quantum correlation in three-level systems (such as the Hanle effect [5], the Autler-Townes effect [6,7], quantum beats [8], coherent population trapping [9,10], electromagnetically induced transparancy (EIT) [11,12], lasing without inversion [13–16], narrowing of the resonant fluorescence spectra [17], tunneling induced transparency [18,19], creation (via spontaneous emission) of the metastable entangled state in a system of two spatially separated atoms in one-dimensional case [20,21], or in a common thermostat [22], and narrowing of the emission spectra in the time delay spectroscopy [23] or due to the correlation measurements [24]).

The matter is, however, that *there are no atoms* where a pair of such close levels (i) exists parallel with the necessary common continuum property (CCP), and (ii) does not involve, in a good approximation, any other decay channels. For example, no splitting like hyperfine, Zeeman, Stark, etc., complies with CCP. Also, none of the above-mentioned interference effects uses a scheme complying with properties (i) and (ii) simultaneously. But, it is not forbidden to think about some artificial systems. One general approach suggested by Agarwal [25] was called "modification of the continuum." As shown in Refs. [26,27] the necessary modification can be achieved using a cavity whose mode frequencies are close to those of transitions from the ground state to the Zeeman sublevels of the excited state. This idea was realized in the experiment of Ref. [28] for the Mössbauer x-ray transition in the ^{57}Fe nuclei.

In our work, a model example of another kind is presented that demonstrates the property announced in the title—but *without* any "modification of the continuum," and also *without* any preliminary (coherent) mixing of the stationary states being a necessary part of the Autler-Townes effect and EIT. The final assembly is shown in Fig. 2. Its constituents are treated in Sec. II. A numerical example is given in Sec. III to show that conditions for a narrow dip effect are reasonable, at least, from the point of view of spectroscopy. Meanwhile, certain factors lead to corrections to Eq. (1). To calculate them a more comprehensive model for a system of two atoms is needed, and this model is solved analytically in Sec. IV— then Eq. (1) becomes a particular case of a more general expression.

*amakarov@isan.troitsk.ru

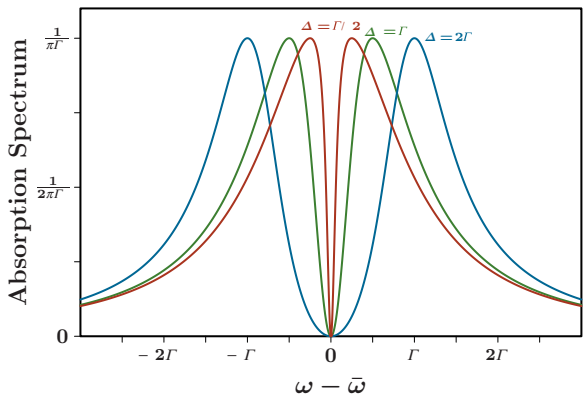

FIG. 1. (Color online) Absorption profiles (1) at $\Gamma_1=\Gamma_2=\Gamma$ and certain values of splitting $\Delta=\omega_{20}-\omega_{10}$ of levels $|1\rangle$ and $|2\rangle$. Parameter $\bar{\omega}$ (2) is equal in this case to the middle frequency $\frac{1}{2}(\omega_{10}+\omega_{20})$.

Substituting the example data of Sec. III into the absorption contour of Sec. IV we, in Sec. V, draw the final spectrum and also present several other examples.

II. QUALITATIVE DISCUSSION AND PRELIMINARY RESULTS

We consider a system of two identical atoms A_1 and A_2 with the ground state $|g\rangle$ and the excited state $|e\rangle$, the distance r between them being less than the allowed transition $|e\rangle\to|g\rangle$ wavelength. Properties of spontaneous emission of this system were studied in numerous works started from that of Dicke [29] (see Ref. [30] for a review and citations therein, and the more recent papers [20,21,31,32]), with an emphasis on the effects of *super-* and *subradiance*. But, properties of absorption (or elastic scattering), as shown in Fig. 1, have not been reported so far.

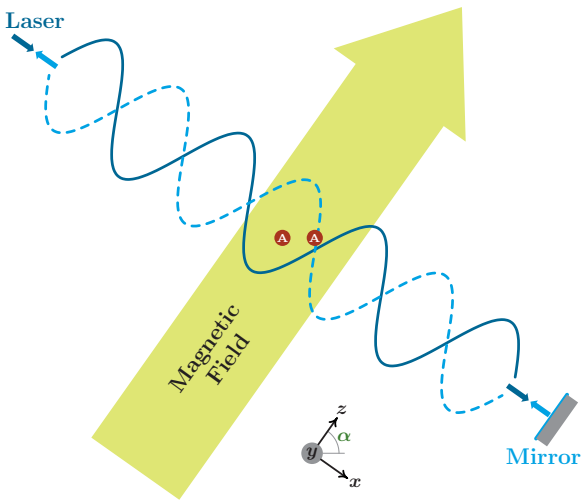

FIG. 2. (Color online) Arrangement of the external fields creating conditions for the effect named in the title. The magnetic field applied at z direction [$\alpha\approx\alpha_0=\arccos(1/\sqrt{3})\approx54.7^\circ$] provides minimization of the dipole-dipole interaction of two identical atoms A. The gradient of electric component $\mathcal{E}\cos k(x-x_0)\cos\omega t$ of the laser field induces a gap between transition frequencies of these atoms. Quantitatively, the magnitude of the magnetic field and the amplitude of the laser field are to provide inequalities given by Eq. (12) below.

The two excited states of the system of two atoms under consideration are $|\mathcal{Q}_1\rangle=|e_1g_2\rangle$ and $|\mathcal{Q}_2\rangle=|g_1e_2\rangle$. Then two factors should be accounted for: the degeneracy that is always present as long as either state $|e\rangle$ or state $|g\rangle$ has a nonzero angular momentum, and the dipole-dipole interaction between the states $|\mathcal{Q}_1\rangle$ and $|\mathcal{Q}_2\rangle$ that, in simple situations, leads to their superpositions producing two *entangled* eigenstates, symmetric and antisymmetric (see, e.g., Refs. [30,33]).

For definiteness, we limit ourselves to a frequent situation where the angular momenta of states $|g\rangle$ and $|e\rangle$ are $J_g=0$ and $J_e=1$, respectively. Then six states are involved in our consideration:

$$\begin{aligned}&\mathcal{Q}_1^{(-1)}=\left|e_1^{(-1)}g_2\right\rangle,\quad \mathcal{Q}_1^{(0)}=\left|e_1^{(0)}g_2\right\rangle,\quad \mathcal{Q}_1^{(+1)}=\left|e_1^{(+1)}g_2\right\rangle,\\ &\mathcal{Q}_2^{(-1)}=\left|g_1e_2^{(-1)}\right\rangle,\quad \mathcal{Q}_2^{(0)}=\left|g_1e_2^{(0)}\right\rangle,\quad \mathcal{Q}_2^{(+1)}=\left|g_1e_2^{(+1)}\right\rangle,\end{aligned}\tag{4}$$

where the upper index indicates the angular-momentum projection M on its quantization axis z. For our purposes, we put the z axis at the so-called *magic angle* $\alpha_0=\arccos(1/\sqrt{3})$ with respect to the vector separation $\mathbf{r}$ between the two atoms. Then the dipole-dipole interaction is represented as

$$\begin{aligned}\widehat{U}&=\frac{(\widehat{\mathbf{d}}_1\cdot\widehat{\mathbf{d}}_2)}{r^3}-3\frac{(\widehat{\mathbf{d}}_1\cdot\mathbf{r})(\widehat{\mathbf{d}}_2\cdot\mathbf{r})}{r^5}\\ &=-\frac{1}{2r^3}[\widehat{d}_1^{(+)}\widehat{d}_2^{(+)}+\widehat{d}_1^{(-)}\widehat{d}_2^{(-)}+\sqrt{2}(\widehat{d}_1^{(+)}+\widehat{d}_1^{(-)})\widehat{d}_2^{(z)}\\ &\quad+\sqrt{2}\,\widehat{d}_1^{(z)}(\widehat{d}_2^{(+)}+\widehat{d}_2^{(-)})],\end{aligned}\tag{5}$$

where the first line (see, e.g., Ref. [34]) does not depend on the choice of the Cartesian coordinates, and the final equality is obtained for $\alpha=\alpha_0$; also, the axis x lies in the plane common with the both z axis and $\mathbf{r}$ vector, and the standard definition $\widehat{d}_{1,2}^{(\pm)}=\widehat{d}_{1,2}^{(x)}\pm i\widehat{d}_{1,2}^{(y)}$ is used for the circular components of the operators $\widehat{\mathbf{d}}_1$ and $\widehat{\mathbf{d}}_2$ of the dipole moment. We note that the unique property of just this representation is that the matrix of the operator $\widehat{U}$ has no couplings between the states (4) with the *same* M, i.e., $\langle\mathcal{Q}_1^{(M)}|\widehat{U}|\mathcal{Q}_2^{(M)}\rangle=0$.

So, to make use of the noted property we add to our composition the magnetic field directed just along the z axis. The aim is to minimize a role of $\widehat{U}$ couplings also between the states with *different* quantum numbers M—and the magnetic field should be strong enough for that. To make estimates it is convenient to express the matrix elements of operator $\widehat{U}$ in terms of two quantities: the rate

$$\Gamma=\frac{32\pi^3}{3\lambda_{eg}^3}|\langle e^{(0)}|\widehat{d}^{(z)}|g\rangle|^2\tag{6}$$

of the spontaneous transition $|e\rangle\to|g\rangle$ where λ_{eg} is its wavelength, and the product kr where $k=2\pi/\lambda_{eg}$. Also, the symmetric $|\mathcal{Q}_\mathrm{s}^{(M)}\rangle=\frac{1}{\sqrt{2}}(\mathcal{Q}_1^{(M)}+\mathcal{Q}_2^{(M)})$ and antisymmetric $|\mathcal{Q}_\mathrm{a}^{(M)}\rangle=\frac{1}{\sqrt{2}}(\mathcal{Q}_1^{(M)}-\mathcal{Q}_2^{(M)})$ superpositions can be used as the basis. Then the matrix $\|U\|$ is separated into two matrices acting independently in the bases of states $|\mathcal{Q}_\mathrm{s}^{(M)}\rangle$ and $|\mathcal{Q}_\mathrm{a}^{(M)}\rangle$,

respectively:

$$\|U_{\rm s}\| = U_r \begin{Vmatrix} 0 & -1 & +1 \\ -1 & 0 & +1 \\ +1 & +1 & 0 \end{Vmatrix}, \qquad \|U_{\rm a}\| = U_r \begin{Vmatrix} 0 & +1 & -1 \\ +1 & 0 & -1 \\ -1 & -1 & 0 \end{Vmatrix}, \tag{7}$$

where $U_r = 3\Gamma/4(kr)^3$, the basis states are enumerated in the ascending order in M, and the standard ratios [35] of the matrix elements $\langle e^{(\pm1)}|\widehat{d}^{(\pm)}|g\rangle$ and $\langle g|\widehat{d}^{(\pm)}|e^{(\mp1)}\rangle$ to the matrix element $\langle e^{(0)}|\widehat{d}^{(z)}|g\rangle$ are used. Now, we add Zeeman splittings of $\pm E_{\rm Z} = \pm\mu_{\rm B} g H$ due to the magnetic field H ($\mu_{\rm B}$ is the Bohr magneton, and g is the Landé g factor) to diagonal zeros of the matrices $U_{\rm s,a}$ in places of states $\mathcal{Q}^{(\pm1)}_{\rm s,a}$, and arrive at the characteristic equations

$$\begin{aligned} \varepsilon_{\rm s}^3 - \left(E_{\rm Z}^2 + 3U_r^2\right)\varepsilon_{\rm s} + 2U_r^3 = 0, \\ \varepsilon_{\rm a}^3 - \left(E_{\rm Z}^2 + 3U_r^2\right)\varepsilon_{\rm a} - 2U_r^3 = 0 \end{aligned} \tag{8}$$

for the energies $\varepsilon_{\rm s}$ and $\varepsilon_{\rm a}$ of our system of two atoms in the magnetic field. These energies are shown in Fig. 3 as functions of the magnetic field. It is seen that, at large magnetic fields, the eigenstates, as can be expected, pair at energies of approximately $\varepsilon \approx \pm E_{\rm Z}$, and $\varepsilon \approx 0$ with small splittings between the symmetric and antisymmetric eigenstates. These splittings, at the condition $E_{\rm Z} \gg U_r$, are

$$\varepsilon_{\rm s} - \varepsilon_{\rm a} \approx \frac{4U_r^3}{E_{\rm Z}^2} \tag{9}$$

at the energy $\varepsilon_{\rm s,a} \approx 0$, and

$$\varepsilon_{\rm s} - \varepsilon_{\rm a} \approx -\frac{2U_r^3}{E_{\rm Z}^2} \tag{10}$$

at the energies $\varepsilon_{\rm s,a} \approx \pm(E_{\rm Z} + 3U_r^2/E_{\rm Z})$. At the same time, the corresponding eigenvectors $|\mathcal{R}^{(M)}_{\rm s,a}\rangle$ are almost $|\mathcal{Q}^{(M)}_{\rm s}\rangle$ and $|\mathcal{Q}^{(M)}_{\rm a}\rangle$, with $M = -1$ at the energy of $\approx -E_{\rm Z}$, $M = 0$ at the zero energy, and $M = +1$ at the energy of $\approx +E_{\rm Z}$. The admixture fractions are shown in Figs. 3(b) and 3(c) as functions of the magnetic field.

So, a strong magnetic field directed at the magic angle can *almost* break the dipole-dipole couplings of two closely spaced atoms, except a very small coupling due to the perturbation of the third order. To cardinally reduce its role one more element is added to our composition that transforms a pair of the symmetric and antisymmetric superpositions $|\mathcal{Q}^{(M)}_{\rm s}\rangle$ and $|\mathcal{Q}^{(M)}_{\rm a}\rangle$ into a pair of the product states $\mathcal{Q}^{(M)}_1 = |e^{(M)}_1 g_2\rangle$ and $\mathcal{Q}^{(M)}_2 = |g_1 e^{(M)}_2\rangle$. Among several possibilities (see a discussion in Sec. VI) we choose (see Fig. 2) a solution as follows. A laser field in a form of standing wave is applied so that its wave vectors $\pm\mathbf{k}_{\rm sw}$ are perpendicular to the magnetic field, and its electric component $\mathcal{E}\cos k_{\rm sw}(x - x_0)\cos\omega_{\rm sw}t$ is directed parallel to the magnetic field. As long as the electric-field amplitudes are *different* in A_1 and A_2 positions the transition frequencies of two atoms undergo *different Stark shifts* $E^{(1)}_{\rm S} \neq E^{(2)}_{\rm S}$. To promote absorption profiles as shown in Fig. 1, their difference

$$\Delta_{\rm S} = \left|E^{(1)}_{\rm S} - E^{(2)}_{\rm S}\right| \tag{11}$$

should be greater than the primary energy splitting (9) or (10), but less than the spontaneous linewidth; i.e., the following

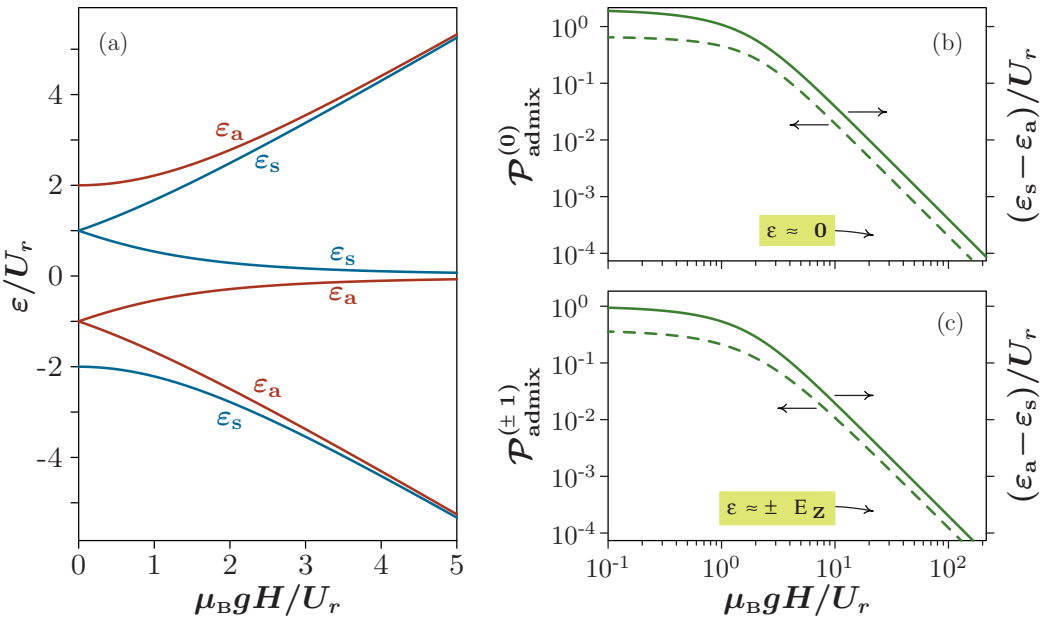

FIG. 3. (Color online) Energies of eigenstates of a system of two atoms as functions of the magnetic field H applied at the magic angle (see Fig. 2). (a) A relatively narrow scale of H variation is presented. (b),(c) A large scale is shown by solid curves for the dependencies of splittings (9) and (10), respectively, on the magnetic field. Also, the fractions of corresponding admixtures defined as $\mathcal{P}^{(M)}_{\rm admix} = \sum_{M'\neq M} |\langle\mathcal{Q}^{(M')}_{\rm s,a}|\mathcal{R}^{(M)}_{\rm s,a}\rangle|^2$ are shown by the dashed curves.

conditions should be valid:

$$\frac{\Gamma^3}{E_Z^2(kr)^9} \ll \Delta_S \lesssim \Gamma, \tag{12}$$

where the U_r definition after Eq. (7) is used.

III. NUMERICAL EXAMPLE

We consider one numerical example. It is optimized from the points of view of spectroscopy and applied fields to show some near-to-maximum characteristics. This example deals with atoms ^{138}Ba having the zero nuclear spin and the ground state $6\,^1S_0$ with the total angular momentum $J_g = 0$. As an excited state, we take $6\,^3P_1$ with $J_e = 1$. The rate of spontaneous transition $6\,^3P_1 \to 6\,^1S_0$ at $\lambda_{eg} \approx 791$ nm is $\Gamma \approx 7.4 \times 10^5\ \mathrm{s}^{-1}$ [36]. Next, for definiteness, we take $kr = 0.25$ (i.e., $r \approx 31.5$ nm) and, to fulfill inequality (12) with a certain reserve, we put $E_Z^2(kr)^9/\Gamma^2 = 10^2$. The latter means that, for our choice of parameters, the Zeeman splitting should be $E_Z = 10\Gamma(kr)^{-4.5} \approx 3.8 \times 10^9\ \mathrm{s}^{-1}$. Taking into account that the Landé g factor for state $^3P_1$ is $g \approx 3/2$ one can find $H \approx 290$ G for the relevant magnetic field. So, at this magnetic field, the residual splitting of the symmetric and antisymmetric eigenstates, say, at zero energy [see Eq. (9)], is $\varepsilon_s - \varepsilon_a \approx (1.7 \times 10^{-2})\Gamma$, i.e., 60 times less than the natural linewidth.

Now, an adequate dynamic range is achieved to follow a dependence of the absorption profile on the difference between Stark shifts of the transition frequencies of two atoms in a laser field of a standing wave as suggested by our scheme in Fig. 2. Although there are different choices of the frequency and polarization of this field we, for definiteness, consider the situation (which may be nonoptimal) where its frequency ω_{sw} is relatively close to that ω_{eg} of our $|e\rangle \to |g\rangle$ transition, but is, at the same time, far enough off the resonance to reduce real excitations to a negligible amount. The interaction with an atom is, as commonly, described by the Rabi frequency $\Omega = d_{eg}\widetilde{\mathcal{E}}/\hbar$, expressed through the amplitude of the laser field $\widetilde{\mathcal{E}}\cos\omega_{sw}t$ at the position of the atom and the corresponding matrix element d_{eg} of the dipole moment, and then inequality $\Omega \ll |\delta|$ must be ensured where $\delta = \omega_{sw} - \omega_{eg}$ (see Fig. 4). In the rotating wave approximation, the Stark shifts of levels $|g\rangle$ and $|e^{(0)}\rangle$ are, respectively, $\pm\frac{1}{2}(\sqrt{\delta^2+\Omega^2} - \delta) \approx \pm\Omega^2/4\delta$. The largest gradient of function $\widetilde{\mathcal{E}}^2 = \mathcal{E}^2\cos^2 k(x - x_0)$ between positions $x_1 = -\frac{1}{2}r\sin\alpha_0$ of atom A_1 and $x_2 = +\frac{1}{2}r\sin\alpha_0$ of atom A_2 is achieved, e.g., at $x_0 = -\frac{1}{8}\lambda_{eg}$. So, for two atoms, the difference of the Stark shifts (that are proportional to the Rabi frequencies squared) is scaled, at our choice of parameters kr and x_0, as $\Delta_S = 2E_S\sin(kr\sin\alpha_0) \approx 0.4E_S$ where E_S is the average shift of transitions $|e_1^{(0)}\rangle \to |g_1\rangle$ and $|e_2^{(0)}\rangle \to |g_2\rangle$, i.e., $E_S \approx -d_{eg}^2\mathcal{E}^2/4\hbar^2\delta$. (See also Fig. 4 for definitions of these quantities.)

Eventually, we use the parameters of two previous paragraphs to calculate the eigenvalues and eigenvectors of the final problem that takes into account the magnetic and laser fields simultaneously. The eigenvalues will give frequencies ω_{10} and ω_{20} for all transitions $|e^{(M)}\rangle \to |g\rangle$, and the eigenvectors will give the corresponding rates Γ_1 and Γ_2; together, they will give all needed parameters to draw the absorption spectrum using

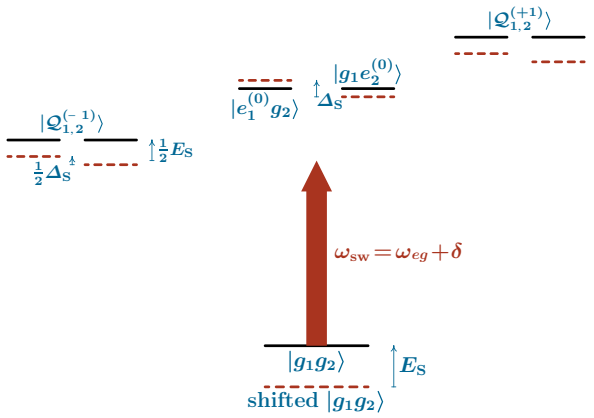

FIG. 4. (Color online) Illustration of the shifts of states (4) by a field different in positions of two atoms. Quantities E_S and Δ_S relate to the shifts of $|e\rangle \to |g\rangle$ transition frequencies. As for the signs of their values, a case is shown where $\delta < 0$, so $E_S > 0$ and $\Delta_S > 0$.

Eq. (1). Calculation results are shown in Fig. 5 for the pair of upper states being basically superpositions of $|e_1^{(0)}g_2\rangle = |\mathcal{Q}_1^{(0)}\rangle$ and $|g_1e_2^{(0)}\rangle = |\mathcal{Q}_2^{(0)}\rangle$ with negligible contributions of the other states. These results coincide very well with simple estimates that can be obtained from the two-level approximation with the interaction matrix $\|Q\|$ that includes Stark shifts $E_S^{(1)}$ and $E_S^{(2)}$ of states $|\mathcal{Q}_1^{(0)}\rangle$ and $|\mathcal{Q}_2^{(0)}\rangle$, respectively, as the diagonal matrix elements, and interaction between them from Eq. (9) and the middle curves in Fig. 3(a), i.e., $\varepsilon_0 = \frac{1}{2}(\varepsilon_s - \varepsilon_a) \approx 2U_r^3/E_Z^2$, as the nondiagonal matrix elements. So, the interaction matrix is

$$\|Q\| = \begin{Vmatrix} E_S^{(1)} & \varepsilon_0 \\ \varepsilon_0 & E_S^{(2)} \end{Vmatrix} \tag{13}$$

that gives for the difference of the eigenvalues

$$\Delta = \omega_{20} - \omega_{10} \approx \sqrt{4\varepsilon_0^2 + \Delta_S^2} \tag{14}$$

where the quantity Δ_S is, as above, the difference (11) of the Stark shifts of the frequencies of transitions $|e_2^{(0)}\rangle \to |g_2\rangle$ and $|e_1^{(0)}\rangle \to |g_1\rangle$. As for the eigenstates of $\|Q\|$, they are

$$\begin{aligned} |1\rangle &= u\big|\mathcal{Q}_1^{(0)}\big\rangle - v\big|\mathcal{Q}_2^{(0)}\big\rangle, \\ |2\rangle &= v\big|\mathcal{Q}_1^{(0)}\big\rangle + u\big|\mathcal{Q}_2^{(0)}\big\rangle \end{aligned} \tag{15}$$

with

$$\begin{aligned} u &= \left\{\frac{1}{2}\left[1 + \frac{\Delta_S}{\left(4\varepsilon_0^2 + \Delta_S^2\right)^{1/2}}\right]\right\}^{1/2}, \\ v &= \left\{\frac{1}{2}\left[1 - \frac{\Delta_S}{\left(4\varepsilon_0^2 + \Delta_S^2\right)^{1/2}}\right]\right\}^{1/2} \end{aligned} \tag{16}$$

where, for definiteness, $\Delta_S > 0$ according to Fig. 4. Hence,

$$\Gamma_{1,2} \approx (u \mp v)^2\Gamma = \Gamma\left(1 \mp \frac{2\varepsilon_0}{\sqrt{4\varepsilon_0^2 + \Delta_S^2}}\right). \tag{17}$$

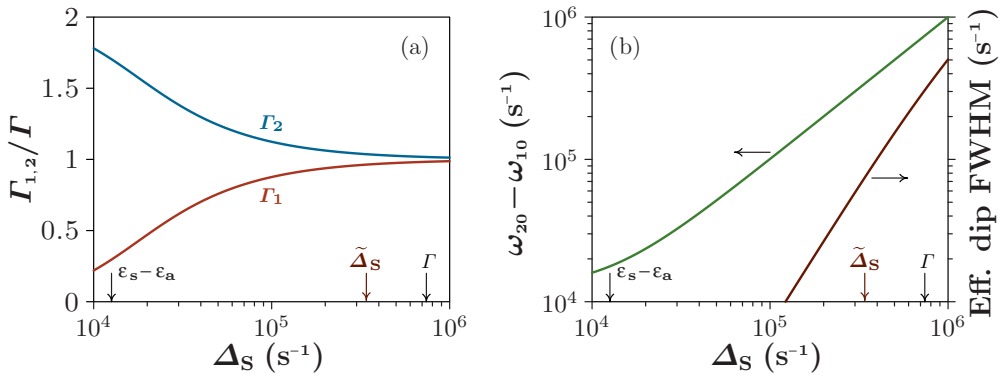

FIG. 5. (Color online) Dependencies of all relevant quantities on the difference of Stark shifts for two states $|1\rangle$ and $|2\rangle$ with $M = 0$. (a) The rates of spontaneous decay starting from $\Gamma_1 \ll \Gamma$ [37] and $\Gamma_2 \approx 2\Gamma$ for, respectively, antisymmetric (*subradiant*) and symmetric (*superradiant*) entangled states approach to Γ as the value of Δ_S grows. (b) Naturally, the splitting between states $|1\rangle$ and $|2\rangle$ and the resulting width of the dip in the absorption profile grow with Δ_S.

Now, the value $\widetilde{\Delta}_S \approx 3.4 \times 10^5$ s^{-1} of the difference of Stark shifts is indicated in Fig. 5 that leads to the width of the dip in the absorption profile ten times less than the natural linewidth. As an example, it is noteworthy to determine characteristics of the standing-wave laser field relating just to this value. The corresponding value of E_S (see Fig. 4 and the accompanying text) is

$$\widetilde{E}_S \approx \frac{d_{eg}^2 \mathcal{E}^2}{4\hbar^2|\delta|} \approx 2.5\widetilde{\Delta}_S \approx 8.5 \times 10^5 \text{ s}^{-1}. \tag{18}$$

It defines options for the input laser intensity $\mathcal{I} = (c/32\pi)\mathcal{E}^2$ and the laser frequency detuning δ. Fixing the value of $\mathcal{I}$ at a moderate level of 10 W/cm^2 we find the required value of the frequency detuning from the resonance with transition $|e\rangle \Leftrightarrow |g\rangle$:

$$|\delta| = \frac{3\Gamma\lambda_{eg}^3\mathcal{I}}{4\pi^2\hbar c\widetilde{E}_S} \approx 10^{11} \text{ s}^{-1}, \tag{19}$$

where Eqs. (6) and (18) are used.

So, an example with realistic spectroscopy and parameters of the applied fields is constructed where a narrow dip in the absorption contour can be expected. In one prominent experiment using EIT, on "storage of light" [38], a full width at half maximum (FWHM) of 40 kHz was observed. In the above example the dip of 7.4×10^4 s$^{-1} \approx 12$ kHz is even narrower [39]. In contrast with the ideal EIT, however, $\mathcal{A} = 0$ at the center here is not an exact result due to the existence of a small additional decay channel. The matter is that the common continuum for two atoms is, in our so-far idealized consideration, associated with the *symmetric* part of $\propto e^{\pm(i/2)\mathbf{kr}}$ atom-field interaction in positions $\pm\frac{1}{2}\mathbf{r}$ of the atoms. Its *antisymmetric* part being proportional to $\pm i \sin\frac{1}{2}\mathbf{kr}$ should be regarded as the other continuum. In terms of the classical electrodynamics, and for the quantization procedure as well, the symmetric and antisymmetric continua are associated with the free-space field modes in a form of standing waves with, respectively, the antinode and the node at $\mathbf{r} = 0$.

To improve Eq. (1) a more general theoretical model is considered below.

IV. TWO DISCRETE STATES AND TWO CONTINUA

A. Formulation of the problem

We consider a problem where two discrete states $|1\rangle$ and $|2\rangle$ with energies E_1 and E_2 are coupled to two common continua of states $|x\rangle$ with energies x and $|y\rangle$ with energies y. No special condition is imposed, at the moment, on couplings of discrete and continuum states—we only introduce two operators $\widehat{F}$ and $\widehat{f}$ (they will be defined below in connection with the problem of the previous sections), and denote the couplings (see Fig. 6) in terms of four *real* functions as

$$\begin{aligned} F_1(x) &= \langle 1|\widehat{F}|x\rangle, \quad F_2(x) = \langle 2|\widehat{F}|x\rangle, \\ f_1(y) &= i\langle 1|\widehat{f}|y\rangle, \quad f_2(y) = -i\langle 2|\widehat{f}|y\rangle, \end{aligned} \tag{20}$$

where $\pm$ signs at i are chosen for further convenience. Also, we require that the integrals of $F_{1,2}^2(x)$ and $f_{1,2}^2(x)$ from $-\infty$ to $+\infty$ are defined. States $|x\rangle$ and $|y\rangle$ are assumed to be normalized to the Dirac δ function, i.e., $\langle x|x'\rangle = \delta(x - x')$ and $\langle y|y'\rangle = \delta(y - y')$. Now, we denote the probability amplitudes

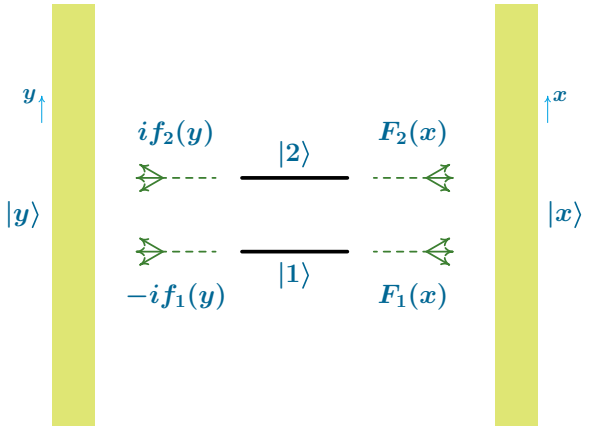

FIG. 6. (Color online) Diagram of states for the problem under treatment in Sec. IV. Interactions of two discrete states $|1\rangle$ and $|2\rangle$ with two continua are described by functions $F_{1,2}(x)$ and $f_{1,2}(y)$. For their general definition, see Eq. (20). Their definition for our system of two atoms in Secs. II and III is given by Eqs. (15), (24), (25), (A5), and (A9).

of the participating states as a_1, a_2, $B(x)$, and $b(y)$, and our task is to determine the energy eigenvalues ω, and the corresponding eigenvectors

$$|\omega\rangle = a_1(\omega)|1\rangle + a_2(\omega)|2\rangle + \int_{x_0}^{\infty} B(x;\omega)|x\rangle\, dx + \int_{y_0}^{\infty} b(y;\omega)|y\rangle\, dy, \tag{21}$$

where x_0 means a boundary of the x continuum or a boundary of the interaction, being formally defined by condition $F_{1,2}(x < x_0) \equiv 0$, and y_0 means the same for the y continuum with condition $f_{1,2}(y < y_0) \equiv 0$. The first task has a trivial solution: the eigenvalue spectrum is *continuous*, i.e., *any* real number between $\min(x_0, y_0)$ and $+\infty$ is an eigenvalue. Moreover, the eigenstates that lie higher than $\max(x_0, y_0)$ are twice degenerate, so *two* eigenvectors $|\omega_{(1)}\rangle$ and $|\omega_{(2)}\rangle$ should be considered. The main part of the problem for the eigenvectors is their *normalization* to the δ function, i.e., should be

$$\begin{aligned} \langle\omega_{(1)}|\omega'_{(1)}\rangle &= \delta(\omega_{(1)} - \omega'_{(1)}), \\ \langle\omega_{(2)}|\omega'_{(2)}\rangle &= \delta(\omega_{(2)} - \omega'_{(2)}), \end{aligned} \tag{22}$$

and their mutual *orthogonalization*, i.e., should be

$$\langle\omega_{(1)}|\omega'_{(2)}\rangle = 0. \tag{23}$$

Equations (22) and (23) are of primary importance for any application.

B. Application

Our application is determination of profile $\mathcal{A}(\omega)$ of the absorption of a tunable monochromatic wave of light—from the ground state $|0\rangle$ in the region of optical transitions $|0\rangle \to |1\rangle$ and $|0\rangle \to |2\rangle$, assuming that there are no other close transitions. In this case (see Appendix A for a more quantitative discussion), the continuum $|x\rangle$ means the direct product states $|0\rangle\otimes|1^{(s)}_x\rangle$ where $|1^{(s)}_x\rangle$ is the symmetric one-photon wave packet of a definite polarization, with the energy measured from $|0\rangle$, so $x_0 = 0$. Continuum $|y\rangle$ means the same, except that a wave packet is antisymmetric. The form of these wave packets depends on polarization. In view of the problem in context [see Fig. 5, Eqs. (14) and (17), and the accompanying text] we are interested in a particular case of optical transitions $M = 0 \leftrightarrow M = 0$ between the ground state and orthogonal superpositions of states $|\mathcal{Q}^{(0)}_1\rangle$ and $|\mathcal{Q}^{(0)}_2\rangle$. These superpositions are defined by Eqs. (15) and (16). Now, as long as the states $|\mathcal{Q}^{(0)}_1\rangle$ and $|\mathcal{Q}^{(0)}_2\rangle$ stand for an atom excitation at coordinates $-\frac{1}{2}\mathbf{r}$ and $+\frac{1}{2}\mathbf{r}$, respectively, their interactions with the antisymmetric continuum of states $|y\rangle$ are of the opposite signs in contrast to their interactions with the symmetric continuum—this approves the notation of Eq. (20). Formulas for the functions $F_{1,2}(x)$ and $f_{1,2}(y)$ include the matrix element $\langle e^{(0)}|\widehat{d}|g\rangle$ of the dipole-moment operator [or the spontaneous decay rate Γ; see Eq. (6)], the mutual orientation of the M quantization axis and vector separation $\mathbf{r}$ (at angle α), Eqs. (15) and (16), and integration over the spherical coordinates θ and φ that takes into account all directions of the wave vector of photons with the same energy. For the transitions with $\Delta M = 0$ (just considered here), those formulas are

$$\begin{aligned} F_1(x) &= (u - v)\,\frac{\sqrt{3\Gamma\Upsilon_c(x)}}{4\pi}, \\ F_2(x) &= (u + v)\,\frac{\sqrt{3\Gamma\Upsilon_c(x)}}{4\pi}, \end{aligned} \tag{24}$$

$$\begin{aligned} f_1(y) &= (u + v)\,\frac{\sqrt{3\Gamma\Upsilon_s(y)}}{4\pi}, \\ f_2(y) &= (u - v)\,\frac{\sqrt{3\Gamma\Upsilon_s(y)}}{4\pi}, \end{aligned} \tag{25}$$

where the functions $\Upsilon_c(x)$ and $\Upsilon_s(y)$ are defined in Appendix A by Eqs. (A9) and (A5).

The absorption spectrum is, by definition, expressed through the matrix elements of the operator of the dipole moment as

$$\mathcal{A}(\omega) \propto |\langle 0|\widehat{d}|\omega_{(1)}\rangle|^2 + |\langle 0|\widehat{d}|\omega_{(2)}\rangle|^2. \tag{26}$$

The same operator of the dipole moment is responsible for the both interaction of the state $|0\rangle$ with the states $|1\rangle$ and $|2\rangle$ and interaction of the states $|1\rangle$ and $|2\rangle$ with the states $|x\rangle$ and $|y\rangle$, so

$$\begin{aligned} \langle 0|\widehat{d}|1\rangle &\propto F_1(\omega_{10}) + i f_1(\omega_{10}), \\ \langle 0|\widehat{d}|2\rangle &\propto F_2(\omega_{20}) - i f_2(\omega_{20}). \end{aligned} \tag{27}$$

Substituting Eq. (21) into each of two terms in Eq. (26) and using Eq. (27) one gets the absorption spectrum as

$$\begin{aligned} \mathcal{A}(\omega) = {} & \frac{1}{F_1^2(\omega) + F_2^2(\omega) + f_1^2(\omega) + f_2^2(\omega)} \\ & \times \sum_{j=1}^{2} \left| [F_1(\omega) + i f_1(\omega)] a_1^{(j)}(\omega) \right. \\ & \left. + [F_2(\omega) - i f_2(\omega)] a_2^{(j)}(\omega) \right|^2, \end{aligned} \tag{28}$$

where the upper index j runs over two degenerate solutions. Provided that the normalization condition (22) and orthogonalization condition (23) are fulfilled, this function $\mathcal{A}(\omega)$ automatically becomes normalized as $\int \mathcal{A}(\omega)\, d\omega = 1$.

A set of equations to determine the eigenvectors follows directly from the Schrödinger equation, being

$$\begin{aligned} (\omega - E_1)\, a_1(\omega) &= \int_0^{\infty} F_1(\xi) B(\xi;\omega)\, d\xi \\ &\quad - i \int_0^{\infty} f_1(\xi) b(\xi;\omega)\, d\xi, \\ (\omega - E_2)\, a_2(\omega) &= \int_0^{\infty} F_2(\xi) B(\xi;\omega)\, d\xi \\ &\quad + i \int_0^{\infty} f_2(\xi) b(\xi;\omega)\, d\xi, \\ (\omega - x) B(x;\omega) &= F_1(x) a_1(\omega) + F_2(x) a_2(\omega), \\ (\omega - y)\, b(y;\omega) &= i f_1(y) a_1(\omega) - i f_2(y) a_2(\omega). \end{aligned} \tag{29}$$

Its solution is presented in Appendix B.

C. General expression for $\mathcal{A}(\omega)$

The absorption spectrum $\mathcal{A}(\omega)$ defined by Eq. (28) is expressed through four functions, namely the eigenvector components $a_1^{(1)}(\omega)$, $a_2^{(1)}(\omega)$, $a_1^{(2)}(\omega)$, and $a_2^{(2)}(\omega)$, where the lower index specifies the discrete state ($|1\rangle$ or $|2\rangle$) and the upper index runs over two orthogonal eigenvectors $|\omega^{(1,2)}\rangle$ attached to eigenvalue ω, as discussed after Eq. (21). These eigenvector components are obtained by combining Eqs. (B4), (B5), (B13), (B14), and (B16). Substituting them into Eq. (28) one arrives at

$$\mathcal{A}(\omega)=\frac{\pi^{-2}}{F_1^2+F_2^2+f_1^2+f_2^2}\left(\frac{\mathcal{R}^{(1)}}{\mathcal{S}+\mathcal{R}^{(1)}}+\frac{\mathcal{R}^{(2)}}{\mathcal{S}+\mathcal{R}^{(2)}}\right), \tag{30}$$

where

$$\mathcal{S}(\omega)=2\mathcal{D}^4+\pi^2\mathcal{D}^2(\mathcal{U}^2+\mathcal{V}^2+2\mathcal{W}^2), \tag{31}$$

$$\begin{aligned}\mathcal{R}^{(1,2)}(\omega)=&\,\pi^2\mathcal{D}^2(\mathcal{U}^2+\mathcal{V}^2+2\mathcal{W}^2)\\&+2\pi^4[\mathcal{U}^2\mathcal{V}^2+(\mathcal{U}^2+\mathcal{V}^2)\mathcal{W}^2+\mathcal{W}^4]\\&\pm 2\pi^2(\mathcal{U}+\mathcal{V})\mathcal{W}[\mathcal{D}^2+\pi^2(\mathcal{U}^2+\mathcal{W}^2)]^{1/2}\\&\times[\mathcal{D}^2+\pi^2(\mathcal{V}^2+\mathcal{W}^2)]^{1/2},\end{aligned} \tag{32}$$

with the functions $\mathcal{U}(\omega)$, $\mathcal{V}(\omega)$, $\mathcal{W}(\omega)$, and $\mathcal{D}(\omega)$ given by Eq. (B14). Furthermore, note that these functions, and $a_{1,2}$ (B5) as well, include quantities $\widetilde{E}_{1,2}(\omega)$ and $\mathcal{I}(\omega)$ defined by Eq. (B4). We will discuss their significance later, first showing the validity of Eq. (1).

D. Derivation of Eq. (1)

A system of two discrete states and *one* continuum being under consideration in Secs. I–III is just a particular case of the general problem solved here—with, e.g., $f_{1,2}=0$. Then $\mathcal{V}=0$, $\mathcal{W}=0$, $\mathcal{S}=2\mathcal{D}^4+\pi^2\mathcal{D}^2\mathcal{U}^2$, and $\mathcal{R}^{(1)}=\mathcal{R}^{(2)}=\pi^2\mathcal{D}^2\mathcal{U}^2$, So,

$$\mathcal{A}(\omega)=\frac{1}{F_1^2+F_2^2}\frac{\mathcal{U}^2}{\mathcal{D}^2+\pi^2\mathcal{U}^2}=\frac{1}{F_1^2+F_2^2}\frac{\left[F_1^2(\omega-\widetilde{E}_2)+F_2^2(\omega-\widetilde{E}_1)+2F_1F_2\mathcal{I}\right]^2}{[(\omega-\widetilde{E}_1)(\omega-\widetilde{E}_2)-\mathcal{I}^2]^2+\pi^2\left[F_1^2(\omega-\widetilde{E}_2)+F_2^2(\omega-\widetilde{E}_1)+2F_1F_2\mathcal{I}\right]^2}. \tag{33}$$

One can ignore dependencies of $F_{1,2}$, $\widetilde{E}_{1,2}$, and $\mathcal{I}$ on ω in Eq. (33); this, at least, for the problem of the present article has a sense, due to the fact that these quantities are constant, of a very big accuracy, on a scale of the width of the absorption profile. Furthermore, the quantities $\int_0^\infty F_i^2(x)/(\omega-x)\,dx$ are usually treated as a part of the Lamb shift of the atomic levels (see, e.g., Ref. [40] and the citations therein), so they can be ignored as soon as the Lamb shift can be beforehand included into the values of energies E_i. These simplifications lead to the Weisskopf-Wigner approximation. Introducing notations $\omega_{10}=\widetilde{E}_1$, $\omega_{20}=\widetilde{E}_2$, and also representing the rates of spontaneous emission as $\Gamma_i=2\pi F_i^2$ in accordance with the Fermi "golden rule," we arrive at

$$\mathcal{A}(\omega)=\frac{1}{2\pi(\Gamma_1+\Gamma_2)}\frac{[\Gamma_1(\omega-\omega_{20})+\Gamma_2(\omega-\omega_{10})+2\sqrt{\Gamma_1\Gamma_2}\mathcal{I}]^2}{[(\omega-\omega_{10})(\omega-\omega_{20})-\mathcal{I}]^2+\frac{1}{4}[\Gamma_1(\omega-\omega_{20})+\Gamma_2(\omega-\omega_{10})+2\sqrt{\Gamma_1\Gamma_2}\mathcal{I}]^2}. \tag{34}$$

So far, when $\mathcal{I}\neq 0$ a difference can be seen between two expressions for $\mathcal{A}(\omega)$, i.e., Eqs. (1) and (34). However, this quantity $\mathcal{I}$ can be excluded due to the following redefinition of the values of ω_{10}, ω_{20}, and the Γ_1/Γ_2 ratio:

$$\omega_{10}^{\rm eff}=\frac{1}{2}[\omega_{10}+\omega_{20}-\sqrt{(\omega_{20}-\omega_{10})^2+4\mathcal{I}^2}],\quad \omega_{20}^{\rm eff}=\frac{1}{2}[\omega_{10}+\omega_{20}+\sqrt{(\omega_{20}-\omega_{10})^2+4\mathcal{I}^2}], \tag{35}$$

$$\begin{aligned}\Gamma_1^{\rm eff}&=\frac{1}{2}\left[\Gamma_1\left(1+\frac{\omega_{20}-\omega_{10}}{\sqrt{(\omega_{20}-\omega_{10})^2+4\mathcal{I}^2}}\right)+\Gamma_2\left(1-\frac{\omega_{20}-\omega_{10}}{\sqrt{(\omega_{20}-\omega_{10})^2+4\mathcal{I}^2}}\right)\right]-\frac{\sqrt{\Gamma_1\Gamma_2}\mathcal{I}}{\sqrt{(\omega_{20}-\omega_{10})^2+4\mathcal{I}^2}},\\ \Gamma_2^{\rm eff}&=\frac{1}{2}\left[\Gamma_1\left(1-\frac{\omega_{20}-\omega_{10}}{\sqrt{(\omega_{20}-\omega_{10})^2+4\mathcal{I}^2}}\right)+\Gamma_2\left(1+\frac{\omega_{20}-\omega_{10}}{\sqrt{(\omega_{20}-\omega_{10})^2+4\mathcal{I}^2}}\right)\right]+\frac{\sqrt{\Gamma_1\Gamma_2}\mathcal{I}}{\sqrt{(\omega_{20}-\omega_{10})^2+4\mathcal{I}^2}},\end{aligned} \tag{36}$$

where $\omega_{20}>\omega_{10}$. With those *effective* values, Eq. (34) takes exactly the form of Eq. (1):

$$\mathcal{A}(\omega)=\frac{1}{2\pi\left(\Gamma_1^{\rm eff}+\Gamma_2^{\rm eff}\right)}\frac{\left[\Gamma_1^{\rm eff}\left(\omega-\omega_{20}^{\rm eff}\right)+\Gamma_2^{\rm eff}\left(\omega-\omega_{10}^{\rm eff}\right)\right]^2}{\left(\omega-\omega_{10}^{\rm eff}\right)^2\left(\omega-\omega_{20}^{\rm eff}\right)^2+\frac{1}{4}\left[\Gamma_1^{\rm eff}\left(\omega-\omega_{20}^{\rm eff}\right)+\Gamma_2^{\rm eff}\left(\omega-\omega_{10}^{\rm eff}\right)\right]^2}. \tag{37}$$

Its universal properties are two equal maximums at $\omega=\omega_{10}^{\rm eff}$ and $\omega=\omega_{20}^{\rm eff}$, and zero $\mathcal{A}$ at $\omega=(\Gamma_1^{\rm eff}\omega_{20}^{\rm eff}+\Gamma_2^{\rm eff}\omega_{10}^{\rm eff})/(\Gamma_1^{\rm eff}+\Gamma_2^{\rm eff})$.

E. Corrections to Eq. (1)

At a small value of the parameter kr a difference between $A(\omega)$ given by Eq. (1) and $A(\omega)$ given by Eqs. (30)–(32) may also be small. To get this difference and include it into the numerical example of Sec. III, a few quantities should be evaluated.

1. Ratio $f^2(\omega_{eg})/F^2(\omega_{eg})$

Discussing the numerical results shown in Fig. 5(a) we have noted that at the left side of the graph (where $\Delta_S\to 0$) the subradiant state with $\Gamma_1\ll\Gamma$ and superradiant state with $\Gamma_2\approx 2\Gamma$ are in play. In view of Eq. (15), this is the simplest case due to $u=v=1/\sqrt{2}$, so $F_1(x)=0$ and $f_2(y)=0$.

Taking the ratio of nonzero f and F, i.e., f_1/F_2, one gets from Eqs. (24), (25), and (A9)

$$\frac{f^2(y=\omega_{eg})}{F^2(x=\omega_{eg})}=\frac{\Upsilon_s(y=\omega_{eg})}{\Upsilon_c(x=\omega_{eg})}=\frac{\int_0^{2\pi}\int_0^{\pi}\sin^2\left[\frac{1}{2}kr(\sin\alpha\sin\theta\cos\varphi+\cos\alpha\cos\theta)\right]\sin^3\theta\,d\theta\,d\varphi}{\int_0^{2\pi}\int_0^{\pi}\cos^2\left[\frac{1}{2}kr(\sin\alpha\sin\theta\cos\varphi+\cos\alpha\cos\theta)\right]\sin^3\theta\,d\theta\,d\varphi}, \tag{38}$$

where $k\equiv\omega_{eg}/c$ by definition. This ratio remains constant at any values of the expansion coefficients u, v (16) in a sense of $(f_1^2+f_2^2)/(F_1^2+F_2^2)$—being equal to the ratio of two rates of the spontaneous decay. At $kr\lesssim 1$ a small rate γ of the decay into the y continuum is expressed through Γ as

$$\gamma\approx\frac{3(kr)^2\Gamma}{32\pi}\int_0^{2\pi}\int_0^{\pi}(\sin\alpha\sin\theta\cos\varphi+\cos\alpha\cos\theta)^2\,d\theta\,d\varphi$$
$$=\frac{1}{8}(kr)^2\Gamma\left[\frac{2}{3}+\frac{1}{5}(2\cos^2\alpha-\sin^2\alpha)\right]. \tag{39}$$

If α is the magic angle α_0 then

$$\gamma\approx\tfrac{1}{12}(kr)^2\Gamma. \tag{40}$$

Hence, an estimate for the rate of spontaneous decay of the subradiant entangled state can also be obtained: it is $2\gamma\approx\frac{1}{6}(kr)^2\Gamma$.

2. *Shifted energies $\widetilde{E}_{1,2}(\omega_{eg})$ and integral $\mathcal{I}(\omega_{eg})$*

These quantities complement each other. Substituting (24) and (25) into Eq. (B4) one arrives at

$$\widetilde{E}_1(\omega_{eg})=E_1+\frac{3\Gamma}{16\pi^2}\fint_0^{\infty}\frac{\frac{3}{8}\pi-2uv[\Upsilon_c(\xi)-\Upsilon_s(\xi)]}{\omega-\xi}\times\mathcal{F}(\xi)d\xi,$$
$$\widetilde{E}_2(\omega_{eg})=E_2+\frac{3\Gamma}{16\pi^2}\fint_0^{\infty}\frac{\frac{3}{8}\pi+2uv[\Upsilon_c(\xi)-\Upsilon_s(\xi)]}{\omega-\xi}\times\mathcal{F}(\xi)\,d\xi,$$
$$\mathcal{I}(\omega_{eg})=\frac{3\Gamma}{16\pi^2}\fint_0^{\infty}\frac{(u^2-v^2)[\Upsilon_c(\xi)-\Upsilon_s(\xi)]}{\omega-\xi}\mathcal{F}(\xi)\,d\xi. \tag{41}$$

Qualitatively these quantities mean the same as explained in Sec. IV D, defining radiative shifts of the levels [see Eq. (35)], and a certain change of the Γ_1/Γ_2 ratio [see Eq. (36)], but their evaluation is more concrete here. So, when $u=1$ and $v=0$ the shifts of levels are equal, whereas the value of $\mathcal{I}$ reaches its maximum value $\mathcal{I}_{\max}$. This occurs in the case where the eigenstates are exactly the pure product states $\mathcal{Q}_1^{(0)}$ and $\mathcal{Q}_2^{(0)}$. In the opposite case, when the eigenstates are the maximally entangled states, i.e., $u=v=1/\sqrt{2}$, then $\mathcal{I}=0$, but the difference of the Lamb shifts of the symmetric $|2\rangle$ and antisymmetric $|1\rangle$ superpositions of $\mathcal{Q}_1^{(0)}$ and $\mathcal{Q}_2^{(0)}$ reaches a value of $2\mathcal{I}_{\max}$. As long as our task is to apply Eqs. (30)–(32) to a situation where states $|1\rangle$ and $|2\rangle$ are almost $|\mathcal{Q}_1^{(0)}\rangle$ and $|\mathcal{Q}_2^{(0)}\rangle$, respectively (see a label $\widetilde{\Delta}_S$ in Fig. 5), we limit ourselves to a case of $F_1(x)\approx F_2(x)$ and $f_1(y)\approx f_2(y)$. Then one has inside the integral $\mathcal{I}$ in the third line of Eq. (41):

$$F_1(\xi)F_2(\xi)-f_1(\xi)f_2(\xi)\approx\frac{3\Gamma\mathcal{F}(\xi)}{16\pi^2}\int_0^{2\pi}\int_0^{\pi}\cos\left[\frac{\xi r}{c}(\sin\alpha\sin\theta\cos\varphi+\cos\alpha\cos\theta)\right]\sin^3\theta\,d\theta\,d\varphi, \tag{42}$$

where the function $\mathcal{F}(\xi)$ is suggested by Eq. (A5) after Ref. [41].

However, the expression (B4) describes only *a part* of interaction between the two atomic states $|eg\rangle$ and $|ge\rangle$ through the electromagnetic field. This part includes just an interaction via the ground state $|gg\rangle$ of the system of two atoms. *Another* part relates to an interaction via the double-excited state $|ee\rangle$. Its addition leads to the following redefinition:

$$\mathcal{I}(\omega_{eg})=\frac{3\Gamma}{16\pi^2}\left\{\int_0^{2\pi}\int_0^{\pi}\sin^3\theta\fint_0^{\infty}\frac{\mathcal{F}(\xi)}{\omega_{eg}-\xi}\cos\left[\frac{\xi r}{c}(\sin\alpha\sin\theta\cos\varphi+\cos\alpha\cos\theta)\right]d\xi\,d\theta\,d\varphi\right.$$
$$\left.-\int_0^{2\pi}\int_0^{\pi}\sin^3\theta\int_0^{\infty}\frac{\mathcal{F}(\xi)}{\omega_{eg}+\xi}\cos\left[\frac{\xi r}{c}(\sin\alpha\sin\theta\cos\varphi+\cos\alpha\cos\theta)\right]d\xi\,d\theta\,d\varphi\right\}$$
$$=\frac{3\Gamma}{16\pi^2}\frac{\omega_{eg}^2+\omega_c^2}{\omega_{eg}}\int_0^{2\pi}\int_0^{\pi}\sin^3\theta\,d\theta\,d\varphi\fint_{-\infty}^{\infty}\frac{\xi\cos[(\xi r/c)(\sin\alpha\sin\theta\cos\varphi+\cos\alpha\cos\theta)]}{(\omega_{eg}-\xi)(\xi^2+\omega_c^2)}d\xi, \tag{43}$$

where the *odd parity* of $\mathcal{F}$ allows us to join the two interaction parts into one analytic integration over the whole real axis ξ. This integration is performed in Appendix C. For the case treated in Secs. I–III, i.e., at the conditions of $kr\ll 1$ and $\alpha=\alpha_0=\arccos(1/\sqrt{3})$ (the magic angle), the calculation gives

$$\mathcal{I}(\omega_{eg})\approx[0.25kr-0.5(kr)^{-1}]\Gamma \tag{44}$$

according to Eqs. (C6) and (C7). It should be noted, however, that this estimate corresponds just to (i) the second order of

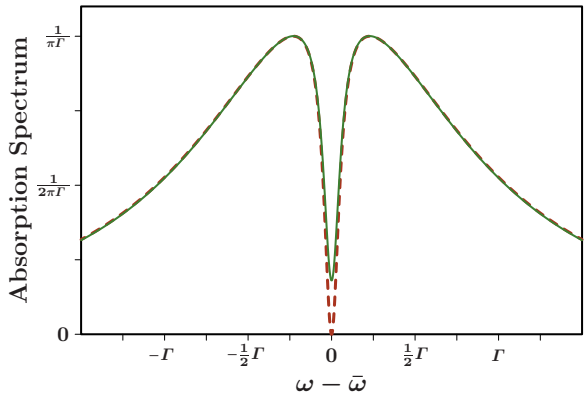

FIG. 7. (Color online) The dashed curve shows the spectrum $\mathcal{A}(\omega)$ [see Eq. (1) with $\Gamma_1 = \Gamma_2 = \Gamma$]. The distance $\Delta \approx 0.46\Gamma$ between the two states is chosen so that the FWHM of $\mathcal{A}(\omega)$ would be equal to $\Gamma/10$. The solid curve takes into account a small correction of Sec. IV E 1 [Eq. (40)] introduced by $\gamma \approx 0.0055$ ($kr = 0.25$ in our numerical example), but ignore corrections of Sec. IV E 2.

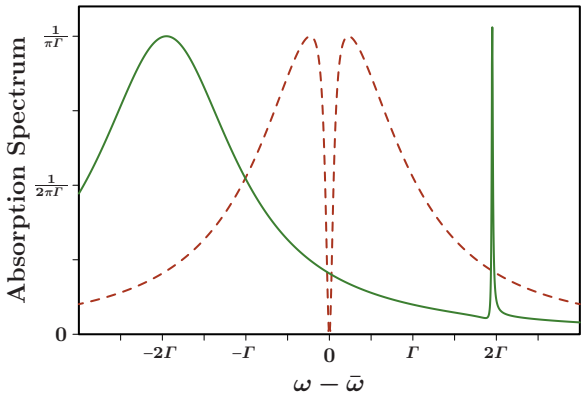

FIG. 8. (Color online) The solid curve shows the spectrum $\mathcal{A}(\omega)$ with inclusion of the quantity $\mathcal{I}$ (44). All other parameters are the same as in Fig. 7. The frequency scale is compressed twice, as compared to that in Fig. 7, and is the same as in Fig. 1.

the perturbation theory, and (ii) our choice of the function $\mathcal{F}$ according to Eq. (A5).

V. FINAL RESULTS

The formulas of Sec. IV and the appendixes are used for calculation of the absorption spectrum for the numerical example of Sec. III. Its difference from the spectrum given by Eq. (1) is determined by two quantities, γ (40) and $\mathcal{I}$ (44), if they are nonzero. First, we analyze separately the role of γ, i.e., the relatively small spontaneous transition rate into the antisymmetric continuum. To do this we put $\mathcal{I} = 0$ in Eq. (B14) and calculate the spectrum using Eqs. (30)–(32) and (40). The result is shown in Fig. 7 by the solid curve. A qualitative property of the improved spectrum is that the additional decay channel lifts $\mathcal{A} = 0$ of Eq. (1) to a nonzero value.

However, the quantity $\mathcal{I}$ dramatically changes the spectrum shape due to that, in the case under consideration, it is of the same order as the total spontaneous decay rate Γ is [see Eq. (44)]. The corresponding absorption spectrum is shown in Fig. 8. Although it has an interesting shape this is not what we want to get. The only way to compensate the repulsing action of $\mathcal{I} \neq 0$ is a slight change of the angle α in Fig. 2 that leads to nonzero matrix elements $\langle \mathcal{Q}_1^{(M)} | \widehat{U} | \mathcal{Q}_2^{(M)} \rangle$ of the operator $\widehat{U}$ of the dipole-dipole interaction. The $\|\widehat{U}_\mathrm{s}\|$ and $\|\widehat{U}_\mathrm{a}\|$ matrices are modified from those given by Eq. (7) to

$$\|U_\mathrm{s}\| = U_r \begin{Vmatrix} 1 - \frac{3}{2}\sin^2\alpha & -\frac{3\sqrt{2}}{4}\sin 2\alpha & \frac{3\sqrt{2}}{4}\sin 2\alpha \\ -\frac{3\sqrt{2}}{4}\sin 2\alpha & 1 - 3\cos^2\alpha & \frac{3\sqrt{2}}{4}\sin 2\alpha \\ \frac{3\sqrt{2}}{4}\sin 2\alpha & \frac{3\sqrt{2}}{4}\sin 2\alpha & 1 - \frac{3}{2}\sin^2\alpha \end{Vmatrix},$$

$$|U_\mathrm{a}\| = U_r \begin{Vmatrix} \frac{3}{2}\sin^2\alpha - 1 & \frac{3\sqrt{2}}{4}\sin 2\alpha & -\frac{3\sqrt{2}}{4}\sin 2\alpha \\ \frac{3\sqrt{2}}{4}\sin 2\alpha & 3\cos^2\alpha - 1 & -\frac{3\sqrt{2}}{4}\sin 2\alpha \\ -\frac{3\sqrt{2}}{4}\sin 2\alpha & -\frac{3\sqrt{2}}{4}\sin 2\alpha & \frac{3}{2}\sin^2\alpha - 1 \end{Vmatrix} \quad (45)$$

for an arbitrary angle α. With a strong magnetic field applied along the axis z, the half splitting between the symmetric and antisymmetric entangled states under consideration, i.e., $\mathcal{Q}_\mathrm{s}^{(0)}$ and $\mathcal{Q}_\mathrm{a}^{(0)}$, is $\approx U_r(1 - 3\cos^2\alpha)$. So, for a compensation of $\mathcal{I}$ at $kr \lesssim 1$, the following condition should be fulfilled:

$$\frac{kr}{4} - \frac{1}{2kr} + \sqrt{2}\left(\frac{kr}{16} + \frac{1}{8kr} + \frac{3}{2(kr)^3}\right)(\alpha - \alpha_0) \ll 10^{-1}. \quad (46)$$

Here, (i) the definition of U_r after Eq. (7) and Eqs. (C6) and (C7) for $\mathcal{I}$ are used, (ii) a small deviation of α from the magic angle α_0 is assumed, and (iii) the compensation accuracy is dictated by a desired width of the dip. Due to a stronger dependence of the dipole-dipole interaction on the parameter kr than the dependence $\mathcal{I}(kr)$, the condition (46) is, indeed, fulfilled at $\alpha - \alpha_0 \ll 1$. Our simulation gives that the transformation of the absorption spectrum in Fig. 8 to

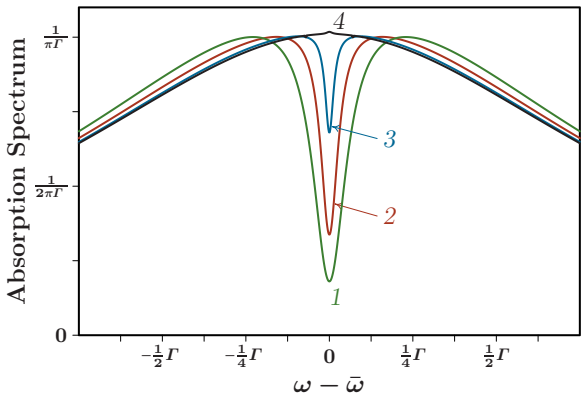

FIG. 9. (Color online) Examples of spectra $\mathcal{A}(\omega)$ calculated using Eqs. (30)–(32) and (39). Equality $\Gamma_1 = \Gamma_2$ and all other conditions of Sec. III are kept. The parameter σ/Γ [see Eq. (3)] that gives an estimate for the dip's relative width is equal to 0.1 (curve 1, same as in Fig. 7), 0.05 (curve 2), 0.02 (curve 3), and 0.01 (curve 4). (The frequency scale is extended twice, as compared to that in Fig. 7, and fourfold, as compared to that in Fig. 8.)

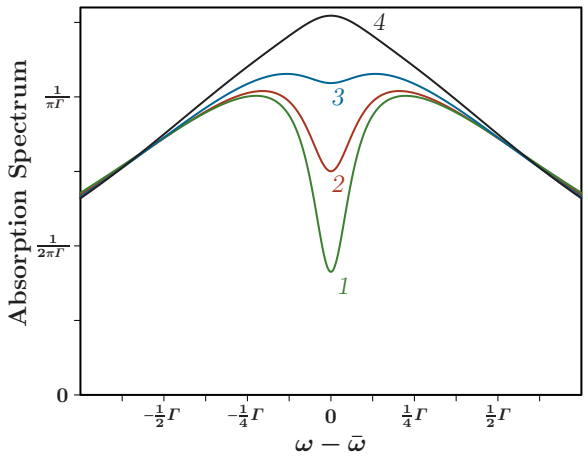

FIG. 10. (Color online) Examples of spectra $\mathcal{A}(\omega)$ calculated using Eqs. (30)–(32) and (39) for different values of the parameter kr at the fixed value of the ratio $\sigma/\Gamma = 0.1$. Curve 1: $kr = 0.4$; 2: $kr = 0.6$; 3: $kr = 0.8$; 4: $kr = 1.0$.

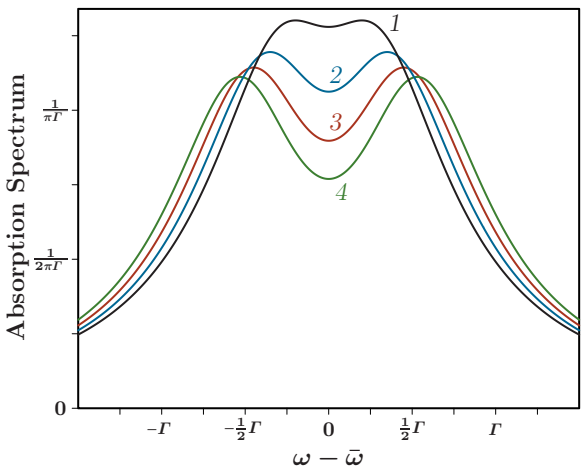

FIG. 11. (Color online) Examples of spectra $\mathcal{A}(\omega)$ calculated using Eqs. (30)–(32) and (39) for different values of the ratio σ/Γ at the fixed value of the parameter $kr = 2.2$. Curve $1 - \sigma = 0.2$; $2 - \sigma = 0.3$; $3 - \sigma = 0.4$; $4 - \sigma = 0.5$.

the spectrum in Fig. 7 is achieved, with a good (about 1%) accuracy, at $\alpha - \alpha_0 \approx 1.4 \times 10^{-2}$ rad $\approx 0.8^\circ$.

A question may be raised about physical limitations on the dip's width. Figure 9 gives a particular answer. Therein, the results of calculation using the formulas of Sec. IV C are shown for the different values of σ given by Eq. (3). It is seen that, with $kr = 0.25$, an attempt to reach a width of about $\Gamma/100$ should not work.

For larger values of kr the limitations are stronger due to an increase of the role of the antisymmetric spontaneous decay [see Eq. (40)], so the dip, even if it exists, is not so pronounced as in Fig. 7. An illustrative example is shown in Fig. 10. Here the desired width of the dip is the same as in Fig. 7 (i.e., $\sigma/\Gamma = 0.1$), and the parameter kr is varied. It is seen that to provide this value of σ the distance r between the atoms should not exceed $\approx \lambda_{eg}/8$.

For every value of the parameter kr a certain critical value of σ exists such as, e.g., $\sigma_{\rm cr} \sim \Gamma/100$ (at $kr = 0.25$) with the upper curve in Fig. 9 where a dip vanishes. Certain results of calculation of these critical values $\sigma_{\rm cr}$ at different kr are presented in Table I. To calculate them suitable angles α were determined using Eqs. (C4), (C7), and an equation like (46) but more accurate; then the corresponding ratios (38) of the two spontaneous decay rates were calculated.

TABLE I. Critical values $\sigma_{\rm cr}$ (fourth column) for different distances between the atoms (first column). Corresponding values of the angle α between the magnetic field and the direction from one atom to another are presented in the second column. Corresponding small fractions of the spontaneous decay into the antisymmetric continuum are presented in the third column.

kr	$\alpha - \alpha_0$ (rad)	$\frac{\gamma}{\Gamma} = \frac{f^2}{F^2+f^2}$	$\sigma_{\rm cr}$
0.25	0.014	0.0052	0.011
0.50	0.051	0.021	0.037
0.75	0.091	0.048	0.073
1.00	0.111	0.084	0.11
1.25	0.090	0.13	0.13
1.50	0.025	0.17	0.14
1.75	−0.073	0.21	0.15
2.00	−0.192	0.24	0.16
2.20	−0.301	0.27	0.16

One can see from the presented results that the raised question about limitations on the dip's width may have a sense just for definite realizations, including a variety of traps for atoms, molecules, or ions, any discussion of which is beyond the scope of this article. We only present one additional example. The last row in Table I is of a special interest for the scheme with two barium atoms introduced in Sec. III. The matter is that the value $kr = 2.2$ exactly corresponds to the distance between the atoms $r \approx 277$ nm that is equal to the half length of the strongest transition $6\,^1S_0 \leftrightarrow 6\,^1P_1$ in the Ba atom. So, it is possible to use trapping of the two atoms in adjacent sites of an optical lattice produced by a laser light with the wavelength near 554 nm. (Such a technology is experimentally approved—for the recent notable achievements see, e.g., Refs. [42,43].) Then the expected absorption spectra at the wavelength of 791 nm are shown in Fig. 11.

VI. CONCLUSIONS

(i) The aim of this article is to show that the effect of the narrow dip within the natural linewidth Γ of the optical transition is possible for a system of two atoms. It is assumed that the distance between the atoms is much smaller than the transition wavelength. Originally any dip narrowness cannot be achieved because the dipole-dipole interaction at so small distances is much larger than Γ so the energies of two excited entangled states $|\mathcal{Q}_{\rm s}^{(M)}\rangle$ and $|\mathcal{Q}_{\rm a}^{(M)}\rangle$ differ much more than the natural linewidth of transition. The basic idea to bring these energies together consists of application of a sufficiently strong magnetic field directed at the magic angle α_0 with respect to the vector separation between the atoms (see Fig. 3). It could

be enough if the atoms were *nonidentical* in a sense that their transition frequencies differ more than the residual splitting of the two entangled states but less than the natural linewidth [see Eq. (12)]. To achieve a *needed difference* of the transition frequencies (so *nonidentity* of the atoms) a scheme using a nonresonant laser standing wave is considered for illustration. One more possible scheme can use a gradient of the magnetic field in the perpendicular direction.

(ii) A model example of Sec. III is chosen to demonstrate conditions for the narrow dip effect that are optimum from the points of view of spectroscopy, applied fields, and the dip's width. In this example, the distance between the atoms is small (dozens of nanometers). For more realistic distances, a dip still exists but it is less pronounced.

(iii) The point concerning an interaction between the excited states of two atoms via the radiation field (integral $\mathcal{I}$ in Sec. IV E 2) has a generic sense. The quantity $\mathcal{I}$ may be treated as a difference between the Lamb shifts (see also Ref. [31]) of the symmetric and antisymmetric entangled states $|\mathcal{Q}_{\rm s}^{(M)}\rangle$ and $|\mathcal{Q}_{\rm a}^{(M)}\rangle$. Its influence on the spectrum is clearly seen by comparing Figs. 7 and 8, but it can be compensated by a small shift of the angle α from α_0. The corresponding data are presented in Table I, but it should be noted that they are calculated just in the second order of the perturbation theory and with a certain model choice of the function $\mathcal{F}$ [see Eq. (A5)]. This point is, probably, worth a further analysis and an experimental test.

(iv) A sensitivity of absorption spectrum to external fields and geometry may be useful for precision measurements and diagnostics.

ACKNOWLEDGMENTS

The work was supported in parts by Russian Foundation for Basic Research Grants No. 13-02-00651a and No. 15-02-05657a. Also, I thank my colleagues in the Institute of Spectroscopy RAS, Y. Lozovik and V. Yudson, for valuable discussions.

APPENDIX A: DETERMINATION OF Υ_c AND Υ_s USED FOR EQS. (24) AND (25)

The atom-field interaction of the product state $|e^{(0)}\rangle\otimes|\text{vac}\rangle$ with the states $|g\rangle\otimes|1^{(0)}_{\xi\mathbf{k}}\rangle$ [where ξ is the frequency of the photon and the superscript (0) points out that the $M=0\to M=0$ transition is just considered] depends on the direction of the photon wave vector $\mathbf{k}$. Let us use a shorter notation for the product states, and denote the corresponding matrix elements as $\beta_{\xi\mathbf{k}}$, or $\beta_\xi(\theta,\varphi)$ where a pair of the spherical angles $\{\theta,\varphi\}$ sets a direction of $\mathbf{k}$. Then it is convenient to use a generic recipe (see, e.g., [44]) enabling us to construct a unique superposition of the states $|g,1^{(0)}_{\xi\theta\varphi}\rangle\equiv|g,1^{(0)}_{\xi\mathbf{k}}\rangle$ that alone interacts with the state $|e^{(0)},\text{vac}\rangle$. Such a superposition can be written as

$$\left|g,1^{(0)}_{\xi}\right\rangle=\frac{\int_0^{2\pi}\int_0^{\pi}\beta_\xi(\theta,\varphi)\left|g,1^{(0)}_{\xi\theta\varphi}\right\rangle\sin\theta\,d\theta\,d\varphi}{\sqrt{\int_0^{2\pi}\int_0^{\pi}|\beta_\xi(\theta,\varphi)|^2\sin\theta\,d\theta\,d\varphi}}. \tag{A1}$$

Next, the interaction of the atom with every plain $\mathbf{k}$ wave is presented (see, e.g., [45,46]) as

$$\widehat{\mathcal{H}}'=\nu\left(\widehat{\mathbf{P}}\cdot\mathbf{e}_{\mathbf{k}\rho}\right)e^{i\mathbf{kR}} \tag{A2}$$

where $\widehat{\mathbf{P}}$ is the operator of the total momentum of electrons, $\mathbf{e}_{\mathbf{k}\rho}$ is the coplanar with $\widehat{\mathbf{P}}$ and perpendicular to the $\mathbf{k}$ unit vector of polarization, $\mathbf{R}$ is the radius vector of the position of the atom. It is convenient to express the proportionality factor ν in Eq. (A2) through the spontaneous emission rate Γ of the transition $|e^{(0)}\rangle\to|g\rangle$ as

$$\nu=\frac{\sqrt{3\Gamma\mathcal{F}(\xi)}}{4\pi|\langle e^{(0)}|\widehat{\mathbf{P}}|g\rangle|} \tag{A3}$$

with $\mathcal{F}(\xi)=1$ at $\xi=\omega_{eg}$. In such a form it complies with the Fermi golden rule,

$$2\pi\left|\langle e^{(0)},\text{vac}\,|\widehat{\mathcal{H}}'\left|g,1^{(0)}_{\omega_{eg}}\right\rangle\right|^2=\Gamma, \tag{A4}$$

since $(\widehat{\mathbf{P}}\cdot\mathbf{e}_{\mathbf{k}\rho})\propto\sin\theta$, and $\int_0^{2\pi}\int_0^{\pi}\sin^3\theta\,d\theta\,d\varphi=8\pi/3$. As for a dimensionless function $\mathcal{F}(\xi)$, it describes a dependence of the atom-field interaction on the photon frequency including the density of the modes of the quantized electromagnetic field. For model estimates of Sec. V E, we choose this function in a form suggested in Ref. [41] as

$$\mathcal{F}(\xi)=\frac{\xi\left(\omega_{eg}^2+\omega_{\rm c}^2\right)}{\omega_{eg}\left(\xi^2+\omega_{\rm c}^2\right)} \tag{A5}$$

with $\omega_c\gg\omega_{eg}$. In addition to (i) the correspondence to the Fermi golden rule at $\xi\approx\omega_{eg}$, this function provides (ii) a simulation of an atom-field interaction in the dipole approximation ($\mathcal{F}\propto\xi$ in a wide range of the photon frequency), and (iii) a smooth cutoff added at $\xi\sim\omega_c\gg\omega_{eg}$ [47,48].

Now we generalize our consideration to the case of two atoms. We adhere to the axis notation shown in Fig. 2, so the two atom radius vectors are $\|R_x=\mp\frac{1}{2}r\sin\alpha, R_y=0, R_z=\mp\frac{1}{2}\cos\alpha\|$, whereas the $\mathbf{k}$ components are $\{k_x=|\mathbf{k}|\sin\theta\cos\varphi, k_y=|\mathbf{k}|\sin\theta\sin\varphi, k_z=|\mathbf{k}|\cos\theta$. Thus, we arrive at

$$\begin{aligned}
\beta_{1\xi}(\theta,\varphi)&\equiv\left\langle e_1^{(0)}g_2,\text{vac}\left|\widehat{\mathcal{H}}'\right|g_1g_2,1^{(0)}_{\xi\theta\varphi}\right\rangle=\frac{\sqrt{3\Gamma\mathcal{F}(\xi)}}{4\pi}\sin\theta\exp\left[-i\,\frac{\xi r}{2c}(\sin\alpha\sin\theta\cos\varphi+\cos\alpha\cos\theta)\right],\\
\beta_{2\xi}(\theta,\varphi)&\equiv\left\langle g_1e_2^{(0)},\text{vac}\left|\widehat{\mathcal{H}}'\right|g_1g_2,1^{(0)}_{\xi\theta\varphi}\right\rangle=\frac{\sqrt{3\Gamma\mathcal{F}(\xi)}}{4\pi}\sin\theta\exp\left[+i\,\frac{\xi r}{2c}(\sin\alpha\sin\theta\cos\varphi+\cos\alpha\cos\theta)\right]
\end{aligned} \tag{A6}$$

for the two atoms, respectively. Hence, one can see that the superpositions (A1) *are different* due to different positions of the atoms. In addition, they are not orthogonal. Thus, it only remains to use separately the real and imaginary parts of the superposition (A1) as *the two states* that uniquely interact with the both atoms—with the same (for the real part) and the opposite (for the imaginary

part) signs of the matrix elements of the atom-field interaction. These two states would be labeled by different frequency variables, e.g., x and y instead of ξ, because they belong, indeed, to *different* continua as shown in Fig. 6. The corresponding formulas for them are

$$\begin{aligned}\left|g_1g_2,1_x^{(0)}\right\rangle &= \sqrt{\frac{3}{8\pi}}\int_0^{2\pi}\int_0^{\pi}\cos\left[\frac{xr}{2c}(\sin\alpha\sin\theta\cos\varphi+\cos\alpha\cos\theta)\right]\sin\theta\left|g_1g_2,1_{x\theta\varphi}^{(0)}\right\rangle\sin\theta\,d\theta\,d\varphi,\\ \left|g_1g_2,1_y^{(0)}\right\rangle &= \sqrt{\frac{3}{8\pi}}\int_0^{2\pi}\int_0^{\pi}\sin\left[\frac{yr}{2c}(\sin\alpha\sin\theta\cos\varphi+\cos\alpha\cos\theta)\right]\sin\theta\left|g_1g_2,1_{x\theta\varphi}^{(0)}\right\rangle\sin\theta\,d\theta\,d\varphi.\end{aligned} \tag{A7}$$

At the end, the final formulas for the matrix elements of the operator $\widehat{\mathcal{H}}'$ are

$$\begin{aligned}\left\langle e_1^{(0)}g_2,\mathrm{vac}\left|\widehat{\mathcal{H}}'\right|g_1g_2,1_x^{(0)}\right\rangle &= \frac{\sqrt{3\Gamma\Upsilon_c(x)}}{4\pi},\quad \left\langle g_1e_2^{(0)},\mathrm{vac}\left|\widehat{\mathcal{H}}'\right|g_1g_2,1_x^{(0)}\right\rangle = \frac{\sqrt{3\Gamma\Upsilon_c(x)}}{4\pi},\\ \left\langle e_1^{(0)}g_2,\mathrm{vac}\left|\widehat{\mathcal{H}}'\right|g_1g_2,1_y^{(0)}\right\rangle &= -i\frac{\sqrt{3\Gamma\Upsilon_s(y)}}{4\pi},\quad \left\langle g_1e_2^{(0)},\mathrm{vac}\left|\widehat{\mathcal{H}}'\right|g_1g_2,1_y^{(0)}\right\rangle = i\frac{\sqrt{3\Gamma\Upsilon_s(y)}}{4\pi},\end{aligned} \tag{A8}$$

where the functions $\Upsilon_c(x)$ and $\Upsilon_s(y)$ are defined as

$$\begin{aligned}\Upsilon_c(x) &= \mathcal{F}(x)\int_0^{2\pi}\int_0^{\pi}\cos^2\left[\frac{xr}{2c}(\sin\alpha\sin\theta\cos\varphi+\cos\alpha\cos\theta)\right]\sin^3\theta\,d\theta\,d\varphi,\\ \Upsilon_s(y) &= \mathcal{F}(y)\int_0^{2\pi}\int_0^{\pi}\sin^2\left[\frac{yr}{2c}(\sin\alpha\sin\theta\cos\varphi+\cos\alpha\cos\theta)\right]\sin^3\theta\,d\theta\,d\varphi.\end{aligned} \tag{A9}$$

APPENDIX B: SOLUTION OF THE EIGENVECTOR PROBLEM (29)

The solution gotten here supplements a collection of analytically solvable "discrete and continuum" models that can be found, e.g., in Refs. [1,2,41,49–51]. The solution is obtained using the distribution approach (distributions are also called generalized functions [52]).

From the last two equations in Eq. (29) one has

$$\begin{aligned}B(x;\omega) &= [F_1(x)a_1(\omega)+F_2(x)a_2(\omega)]\mathcal{P}\frac{1}{\omega-x}\\ &\quad+G(\omega)\delta(\omega-x),\\ b(y;\omega) &= i[f_1(y)a_1(\omega)-f_2(y)a_2(\omega)]\mathcal{P}\frac{1}{\omega-y}\\ &\quad+g(\omega)\delta(\omega-y),\end{aligned} \tag{B1}$$

where $G(\omega)$ and $g(\omega)$ are arbitrary constants for each twice degenerate ω eigenvalue. The two distributions, $\delta(\omega-\xi)$ and $\mathcal{P}\frac{1}{\omega-\xi}$ ($\xi\equiv x,y$), enter Eq. (B1). They are defined as functionals

$$\begin{aligned}(\delta(\omega-\xi),\phi(\xi)) &= \int_{-\infty}^{\infty}\phi(\xi)\delta(\omega-\xi)\,d\xi\equiv\phi(\omega),\\ \left(\mathcal{P}\frac{1}{\omega-\xi},\phi(\xi)\right) &= \mathsf{Vp}\int_{-\infty}^{\infty}\frac{\phi(\xi)}{\omega-\xi}\,d\xi\equiv\fint_{-\infty}^{\infty}\frac{\phi(\xi)}{\omega-\xi}\,d\xi\end{aligned} \tag{B2}$$

acting in a space of trial functions ϕ that rapidly fall at the infinity. (The slash means the same as "Vp"—that the integral is understood in the sense of its *Valeur principale* (principal value) of Augustin-Louis Cauchy.) Next, we put (B1) in the first two equations (29) and arrive at the following set of equations for $a_{1,2}(\omega)$:

$$\begin{aligned}&(\omega-\widetilde{E}_1(\omega))a_1(\omega)-\mathcal{I}(\omega)a_2(\omega)\\ &\quad=F_1(\omega)G(\omega)-if_1(\omega)g(\omega)\\ &-\mathcal{I}(\omega)a_1(\omega)+(\omega-\widetilde{E}_2(\omega))a_2(\omega)\\ &\quad=F_2(\omega)G(\omega)+if_2(\omega)g(\omega),\end{aligned} \tag{B3}$$

where

$$\begin{aligned}\widetilde{E}_i(\omega) &= E_i+\int_0^{\infty}\frac{F_i^2(\xi)+f_i^2(\xi)}{\omega-\xi}\,d\xi,\\ \mathcal{I}(\omega) &= \fint_0^{\infty}\frac{F_1(\xi)F_2(\xi)-f_1(\xi)f_2(\xi)}{\omega-\xi}\,d\xi.\end{aligned} \tag{B4}$$

Hence we get

$$\begin{aligned}a_1 &= \frac{(F_1G-if_1g)(\omega-\widetilde{E}_2)+(F_2G+if_2g)\mathcal{I}}{(\omega-\widetilde{E}_1)(\omega-\widetilde{E}_2)-\mathcal{I}^2},\\ a_2 &= \frac{(F_2G+if_2g)(\omega-\widetilde{E}_1)+(F_1G-if_1g)\mathcal{I}}{(\omega-\widetilde{E}_1)(\omega-\widetilde{E}_2)-\mathcal{I}^2},\end{aligned} \tag{B5}$$

where bracketed ω is omitted for shortness. As a final step, it is required to determine G and g as functions of ω. To do this one has to use normalization and orthogonalization conditions (22) and (23), respectively. Rewriting them in an explicit form with the use of Eq. (21) as

$$\begin{aligned}&a_1^{(j)}(\omega)a_1^{(j)*}(\omega')+a_2^{(j)}(\omega)a_2^{(j)*}(\omega')\\ &\quad+\int_0^{\infty}B^{(j)}(x;\omega)B^{(j)*}(x;\omega')\,dx\\ &\quad+\int_0^{\infty}b^{(j)}(y;\omega)b^{(j)*}(y;\omega')\,dy=\delta(\omega-\omega')\end{aligned} \tag{B6}$$

and

$$a_1^{(1)}(\omega)a_1^{(2)*}(\omega') + a_2^{(1)}(\omega)a_2^{(2)*}(\omega') + \int_0^\infty B^{(1)}(x;\omega)B^{(2)*}(x;\omega')\,dx + \int_0^\infty b^{(1)}(y;\omega)b^{(2)*}(y;\omega')\,dy = 0, \tag{B7}$$

one can see a necessity for additional definitions, namely, what do the three integrals mean? Those integrals are

$$\mathcal{J}_1 = \int_0^\infty \delta(\omega-\xi)\delta(\omega'-\xi)\,d\xi = ?,$$
$$\mathcal{J}_2 = \int_0^\infty \mathcal{G}(\xi;\omega)\mathcal{P}\frac{1}{\omega-\xi}\delta(\omega'-\xi)\,d\xi = ?, \tag{B8}$$
$$\mathcal{J}_3 = \int_0^\infty \mathcal{G}(\xi;\omega)\mathcal{P}\frac{1}{\omega-\xi}\mathcal{G}(\xi;\omega')\mathcal{P}\frac{1}{\omega'-\xi}\,d\xi = ?$$

with function $\mathcal{G}$ either $\mathcal{G}(\xi;\omega) = F_1(\xi)a_1(\omega) + F_2(\xi)a_2(\omega)$ or $\mathcal{G}(\xi;\omega) = f_1(\xi)a_1(\omega) - f_2(\xi)a_2(\omega)$ where $a_{1,2}$ are defined by Eq. (B5). These integrals should be treated as the distributions, i.e., functionals like (B2) acting on the trial functions ϕ. This task is easy for the first two integrals:

$$\mathcal{J}_1(\omega,\omega') = \delta(\omega-\omega'),$$
$$\mathcal{J}_2(\omega,\omega') = \mathcal{G}(\omega',\omega)\mathcal{P}\frac{1}{\omega-\omega'}. \tag{B9}$$

The third integral in Eq. (B8) can be transformed to a combination of the known distributions with the use of the formula of Sokhotsky [53]. It represents the principal-value distribution as

$$\mathcal{P}\frac{1}{\omega-\xi} = i\pi\delta(\omega-\xi) + \lim_{\epsilon\to+0}\frac{1}{\omega-\xi+i\epsilon}. \tag{B10}$$

Hence, using also Eq. (B9), we have

$$\begin{aligned}
\mathcal{J}_3(\omega,\omega') &= i\pi\int_0^\infty \delta(\omega-\xi)\mathcal{G}(\xi;\omega)\mathcal{G}(\xi;\omega')\mathcal{P}\frac{1}{\omega'-\xi}\,d\xi + \lim_{\epsilon\to+0}\int_0^\infty \frac{\mathcal{G}(\xi;\omega)\mathcal{G}(\xi;\omega')}{(\omega-\xi+i\epsilon)(\omega'-\xi)}\,d\xi \\
&= i\pi\mathcal{G}(\omega,\omega)\mathcal{G}(\omega,\omega')\mathcal{P}\frac{1}{\omega'-\omega} + \left(\lim_{\epsilon\to+0}\frac{1}{\omega-\omega'+i\epsilon}\right)\left(\int_0^\infty \frac{\mathcal{G}(\xi;\omega)\mathcal{G}(\xi;\omega')}{\omega'-\xi}\,d\xi - \lim_{\epsilon\to+0}\int_0^\infty \frac{\mathcal{G}(\xi;\omega)\mathcal{G}(\xi;\omega')}{\omega-\xi+i\epsilon}\,d\xi\right) \\
&= i\pi\mathcal{G}(\omega,\omega)\mathcal{G}(\omega,\omega')\mathcal{P}\frac{1}{\omega'-\omega} \\
&\quad + \left(\mathcal{P}\frac{1}{\omega-\omega'} - i\pi\delta(\omega-\omega')\right)\left[\int_0^\infty \frac{\mathcal{G}(\xi;\omega)\mathcal{G}(\xi;\omega')}{\omega'-\xi}\,d\xi - \int_0^\infty \mathcal{G}(\xi;\omega)\mathcal{G}(\xi;\omega')\left(\mathcal{P}\frac{1}{\omega-\xi} - i\pi\delta(\omega-\xi)\right)d\xi\right] \\
&= \pi^2\mathcal{G}^2(\omega,\omega)\delta(\omega-\omega') + \mathcal{P}\frac{1}{\omega-\omega'}\int_0^\infty \frac{\mathcal{G}(\xi;\omega)\mathcal{G}(\xi;\omega')}{\omega'-\xi}\,d\xi + \mathcal{P}\frac{1}{\omega'-\omega}\int_0^\infty \frac{\mathcal{G}(\xi;\omega)\mathcal{G}(\xi;\omega')}{\omega-\xi}\,d\xi.
\end{aligned} \tag{B11}$$

Everything is ready now to get $G(\omega)$ and $g(\omega)$. Roughly, the terms of two types appear as a result of substitution of Eqs. (B1) and (B5) into Eqs. (B6) and (B7) with the use of Eqs. (B8), (B9), and (B11). First, one can extract the terms that are proportional to the δ function. Second, it can be found that all other terms are mutually canceled. It is convenient to begin with the orthogonalization condition. It should be

$$\begin{aligned}
&\pi^2\left(F_1a_1^{(1)} + F_2a_2^{(1)}\right)\left(F_1a_1^{(2)*} + F_2a_2^{(2)*}\right) + G^{(1)}G^{(2)*} + \pi^2\left(f_1a_1^{(1)} - f_2a_2^{(1)}\right)\left(f_1a_1^{(2)*} - f_2a_2^{(2)*}\right) + g^{(1)}g^{(2)*} \\
&= G^{(1)}G^{(2)*}\left\{1 + \frac{\pi^2}{[(\omega-\widetilde{E}_1)(\omega-\widetilde{E}_2) - \mathcal{I}^2]^2}\left([F_1^2(\omega-\widetilde{E}_2) + F_2^2(\omega-\widetilde{E}_1) + 2F_1F_2\mathcal{I}]^2\right.\right. \\
&\quad \left.\left. + [F_1f_1(\omega-\widetilde{E}_2) - F_2f_2(\omega-\widetilde{E}_1) + (F_2f_1 - F_1f_2)\mathcal{I}]^2\right)\right\} \\
&\quad + g^{(1)}g^{(2)*}\left\{1 + \frac{\pi^2}{[(\omega-\widetilde{E}_1)(\omega-\widetilde{E}_2) - \mathcal{I}^2]^2}\left([f_1^2(\omega-\widetilde{E}_2) + f_2^2(\omega-\widetilde{E}_1) - 2f_1f_2\mathcal{I}]^2\right.\right. \\
&\quad \left.\left. + [F_1f_1(\omega-\widetilde{E}_2) - F_2f_2(\omega-\widetilde{E}_1) + (F_2f_1 - F_1f_2)\mathcal{I}]^2\right)\right\} \\
&\quad + (G^{(1)}g^{(2)*} - g^{(1)}G^{(2)*})\frac{i\pi^2[F_1f_1(\omega-\widetilde{E}_2) - F_2f_2(\omega-\widetilde{E}_1) + (F_2f_1 - F_1f_2)\mathcal{I}]}{[(\omega-\widetilde{E}_1)(\omega-\widetilde{E}_2) - \mathcal{I}^2]^2} \\
&\quad \times\left\{\left[F_1^2(\omega-\widetilde{E}_2) + F_2^2(\omega-\widetilde{E}_1) + 2F_1F_2\mathcal{I}\right]^2 + \left[f_1^2(\omega-\widetilde{E}_2) + f_2^2(\omega-\widetilde{E}_1) - 2f_1f_2\mathcal{I}\right]^2\right\} = 0,
\end{aligned} \tag{B12}$$

where the first line is combination of Eqs. (B1), (B7), (B9), and (B11), and the final equality is a result of substitution of Eq. (B5) into the first line. To satisfy Eq. (B12) the easiest choice for $G^{(1,2)}$ and $g^{(1,2)}$ is (from a number of choices) the following:

$$\begin{aligned} G^{(1)} &= \mathcal{C}^{(1)}\left(1+\pi^2\frac{\mathcal{V}^2+\mathcal{W}^2}{\mathcal{D}^2}\right)^{1/2}, \\ g^{(1)} &= i\,\mathcal{C}^{(1)}\left(1+\pi^2\frac{\mathcal{U}^2+\mathcal{W}^2}{\mathcal{D}^2}\right)^{1/2}, \\ G^{(2)} &= \mathcal{C}^{(2)}\left(1+\pi^2\frac{\mathcal{V}^2+\mathcal{W}^2}{\mathcal{D}^2}\right)^{1/2}, \\ g^{(2)} &= -i\,\mathcal{C}^{(2)}\left(1+\pi^2\frac{\mathcal{U}^2+\mathcal{W}^2}{\mathcal{D}^2}\right)^{1/2}, \end{aligned} \tag{B13}$$

where the following notation is used for shortness:

$$\begin{aligned} \mathcal{D} &= (\omega-\widetilde{E}_1)(\omega-\widetilde{E}_2)-\mathcal{I}^2, \\ \mathcal{U} &= F_1^2(\omega-\widetilde{E}_2)+F_2^2(\omega-\widetilde{E}_1)+2F_1F_2\mathcal{I}, \\ \mathcal{V} &= f_1^2(\omega-\widetilde{E}_2)+f_2^2(\omega-\widetilde{E}_1)-2f_1f_2\mathcal{I}, \\ \mathcal{W} &= F_1f_1(\omega-\widetilde{E}_2)-F_2f_2(\omega-\widetilde{E}_1)+(F_2f_1-F_1f_2)\mathcal{I}, \end{aligned} \tag{B14}$$

and real functions $C^{(1)}(\omega)$ and $C^{(2)}(\omega)$ serve as the normalization constants, at a given eigenvalue ω, for the two orthogonal eigenvectors according to Eq. (B6). The normalization condition on $\mathcal{C}^{(1,2)}$ follows from

$$G^2+|g|^2+\pi^2(F_1a_1+F_2a_2)^2+\pi^2(f_1a_1-f_2a_2)^2=1. \tag{B15}$$

Hence

$$\begin{aligned} \frac{\mathcal{D}^4}{(\mathcal{C}^{(1,2)})^2} &= 2\mathcal{D}^4+2\pi^2\mathcal{D}^2(\mathcal{U}^2+\mathcal{V}^2+2\mathcal{W}^2) \\ &\quad +2\pi^4[\mathcal{U}^2\mathcal{V}^2+(\mathcal{U}^2+\mathcal{V}^2)\mathcal{W}^2+\mathcal{W}^4] \\ &\quad \pm 2\pi^2(\mathcal{U}+\mathcal{V})\mathcal{W}[\mathcal{D}^2+\pi^2(\mathcal{U}^2+\mathcal{W}^2)]^{1/2} \\ &\quad \times[\mathcal{D}^2+\pi^2(\mathcal{V}^2+\mathcal{W}^2)]^{1/2}. \end{aligned} \tag{B16}$$

All necessary formulas to determine the absorption spectrum are given in the beginning of Sec. IV C with references to the formulas of this Appendix.

APPENDIX C: CALCULATION OF THE INTEGRAL (43)

The integration in the variable ξ in Eq. (43) gives

$$\begin{aligned} \fint_{-\infty}^{\infty}\frac{\xi\cos[(\xi r/c)(\sin\alpha\sin\theta\cos\varphi+\cos\alpha\cos\theta)]}{(\omega_{eg}-\xi)(\xi^2+\omega_c^2)}\,d\xi &= \mathrm{Re}\fint_{-\infty}^{\infty}\frac{\xi\exp[i(\xi r/c)|\sin\alpha\sin\theta\cos\varphi+\cos\alpha\cos\theta|]}{(\omega_{eg}-\xi)(\xi^2+\omega_c^2)}\,d\xi \\ &= \mathrm{Re}\left[\pi i\operatorname*{Res}_{\xi=\omega_{eg}}I(\xi)+2\pi i\operatorname*{Res}_{\xi=i\omega_c}I(\xi)\right], \end{aligned} \tag{C1}$$

where $I(\xi)$ is the integrand in the right side of the first line. The residues in the second line are

$$\operatorname*{Res}_{\xi=\omega_{eg}}I(\xi)=-\frac{\omega_{eg}}{\omega_{eg}^2+\omega_c^2}\times\exp(ikr|\sin\alpha\sin\theta\cos\varphi+\cos\alpha\cos\theta|) \tag{C2}$$

with $k=\omega_{eg}/c$ by definition, and

$$\operatorname*{Res}_{\xi=i\omega_c}I(\xi)=\frac{1}{2(\omega_{eg}-i\omega_c)}\times\exp\left(-\frac{\omega_c r}{c}|\sin\alpha\sin\theta\cos\varphi+\cos\alpha\cos\theta|\right). \tag{C3}$$

Hence, for the whole integral (43) we have $\mathcal{I}(\omega_{eg})=\mathcal{I}'(\omega_{eg})+\mathcal{I}''(\omega_{eg})$ with

$$\mathcal{I}'(\omega_{eg})=\frac{3\Gamma}{16\pi}\int_0^{2\pi}\int_0^{\pi}\sin(kr|\sin\alpha\sin\theta\cos\varphi+\cos\alpha\cos\theta|)\sin^3\theta\,d\theta\,d\varphi, \tag{C4}$$

$$\mathcal{I}''(\omega_{eg})=-\frac{3\Gamma}{16\pi}\frac{\omega_c}{\omega_{eg}}\int_0^{2\pi}\int_0^{\pi}\exp\left(-\frac{\omega_c r}{c}|\sin\alpha\sin\theta\cos\varphi+\cos\alpha\cos\theta|\right)\sin^3\theta\,d\theta\,d\varphi. \tag{C5}$$

In particular, at $kr\lesssim 1$ the integration for the first term gives

$$\begin{aligned} \mathcal{I}'(\omega_{eg}) &\approx \frac{3kr\Gamma}{16\pi}\int_0^{2\pi}d\varphi\left(\int_0^{\theta_0(\varphi)}(\sin\alpha\sin\theta\cos\varphi+\cos\alpha\cos\theta)\sin^3\theta\,d\theta-\int_{\theta_0(\varphi)}^{\pi}(\sin\alpha\sin\theta\cos\varphi+\cos\alpha\cos\theta)\sin^3\theta\,d\theta\right) \\ &= \frac{3kr\Gamma}{16\pi}\left\{\frac{1}{2}\cos\alpha\int_0^{2\pi}\sin^4\theta_0(\varphi)\,d\varphi\right. \\ &\quad \left.+\sin\alpha\int_0^{2\pi}\left[-\frac{3\pi}{8}+\frac{3}{4}\theta_0(\varphi)-\sin\theta_0(\varphi)\cos\theta_0(\varphi)+\frac{1}{4}\sin\theta_0(\varphi)\cos^3\theta_0(\varphi)-\frac{1}{4}\sin^3\theta_0(\varphi)\cos\theta_0(\varphi)\right]\cos\varphi\,d\varphi\right\} \\ &\equiv \frac{3kr\Gamma}{16\pi}\left(\cos\alpha+\frac{3\sin^2\alpha}{2\cos\alpha}\right)\int_{-\infty}^{\infty}\frac{dx}{1+\tan^2\alpha+x^2}=\frac{3kr\Gamma}{16}\left(1+\frac{1}{2}\sin^2\alpha\right), \end{aligned} \tag{C6}$$

where $\theta_0(\varphi)$ corresponds to the zero value of the integrand, so that $\sin\theta_0(\varphi)=(1+\tan^2\alpha\cos^2\varphi)^{-1/2}$ and $\cos\theta_0(\varphi)=-\tan\alpha\cos\varphi(1+\tan^2\alpha\cos^2\varphi)^{-1/2}$, and the standard variable substitution $x=\tan\varphi$ is used. For the second term $\mathcal{I}''$, just a

small part of the integration region is significant due to a strong inequality $\omega_c r/c \gg 1$. This part is localized along the above introduced curve $\theta_0(\varphi)$ in the plane of the variables $\{\theta,\varphi\}$. This curve is exactly the above introduced $\theta_0(\varphi)$ where the sharp maximum of the integrand is reached. So, the value of the integral in $\mathcal{I}''$ (C5) in the variable θ can be approximated using the derivative at θ_0 and extending the integration into the whole axis. As a result one can get

$$\mathcal{I}''(\omega_{eg}) \approx -\frac{3\Gamma}{16\pi}\frac{\omega_c}{\omega_{eg}}\int_0^{2\pi}\sin^3\theta_0(\varphi)\int_{-\infty}^{\infty}\exp\left(-\frac{\omega_c r}{c}\left|\frac{\partial}{\partial\theta}(\sin\alpha\sin\theta\cos\varphi+\cos\alpha\cos\theta)|_{\theta=\theta_0(\varphi)}[\theta-\theta_0(\varphi)]\right|\right)d\theta\,d\varphi$$
$$= -\frac{3\Gamma}{8\pi kr\cos\alpha}\int_0^{2\pi}\frac{d\varphi}{(1+\tan^2\alpha\cos^2\varphi)^2} = -\frac{3\Gamma}{8kr}(1+\cos^2\alpha). \tag{C7}$$

Notice that (i) the value of the cutoff frequency ω_c does not enter Eq. (C7), and (ii) the two contributions $\mathcal{I}'$ and $\mathcal{I}''$ are of the opposite signs, so they can interfere. These points are discussed in Secs. IV E 2 and V.

[1] U. Fano, Phys. Rev. **124**, 1866 (1961). See Sec. 5 of this paper.
[2] C. Cohen-Tannoudji, J. Dupont-Roc, and G. Grynberg, *Atom-Photon Interactions: Basic Processes and Applications* (Wiley, New York, 1992), pp. 64–66.
[3] V. Weisskopf and E. Wigner, Z. Phys. **63**, 54 (1930).
[4] P. Zhou and S. Swain, Phys. Rev. Lett. **78**, 832 (1997).
[5] W. Hanle, Z. Phys. **30**, 93 (1924).
[6] S. R. Autler and C. R. Townes, Phys. Rev. **100**, 703 (1955).
[7] J. L. Picqué and J. Pinard, J. Phys. B **9**, L77 (1976).
[8] E. B. Aleksandrov, Opt. Spectrosc. **17**, 522 (1964).
[9] G. Alzetta, A. Gozzini, L. Moi, and G. Orriols, Nuovo Cimento B **36**, 5 (1976).
[10] E. Arimondo, in *Progress in Optics XXXV*, edited by E. Wolf (Elsevier Science B. V., Amsterdam, 1996), p. 259.
[11] K.-J. Boller, A. Imamoglu, and S. E. Harris, Phys. Rev. Lett. **66**, 2593 (1991).
[12] M. Fleischhauer, A. Imamoglu, and J. P. Marangos, Rev. Mod. Phys. **77**, 633 (2005).
[13] O. Kocharovskaya and Ya. I. Khanin, JETP Lett. **48**, 630 (1988).
[14] S. E. Harris, Phys. Rev. Lett. **62**, 1033 (1989).
[15] M. O. Scully, S.-Y. Zhu, and A. Gavrielides, Phys. Rev. Lett. **62**, 2813 (1989).
[16] A. Nottelmann, C. Peters, and W. Lange, Phys. Rev. Lett. **70**, 1783 (1993).
[17] P. Zhou and S. Swain, Phys. Rev. Lett. **77**, 3995 (1996).
[18] H. Schmidt, K. L. Campman, A. C. Gossard, and A. Imamoğlu, Appl. Phys. Lett. **70**, 3455 (1997).
[19] T. Wang, R. Zhang, C. Zhou, and X. Su, Opt. Photon. J. **03**, 293 (2013).
[20] A. A. Makarov and V. S. Letokhov, JETP **97**, 688 (2003).
[21] E. S. Redchenko and V. I. Yudson, Phys. Rev. A **90**, 063829 (2014).
[22] A. M. Basharov, JETP **94**, 1070 (2002).
[23] P. Meystre, M. O. Scully, and H. Walther, Opt. Commun. **33**, 153 (1980).
[24] M. O. Scully, U. W. Rathe, Chang Su, and G. S. Agarwal, Opt. Commun. **136**, 39 (1997).
[25] G. S. Agarwal, Phys. Rev. Lett. **84**, 5500 (2000).
[26] A. K. Patnaik and G. S. Agarwal, Phys. Rev. A **59**, 3015 (1999).
[27] P. Zhou and S. Swain, Opt. Commun. **179**, 267 (2000).
[28] K. P. Heeg, H.-C. Wille, K. Schlage, T. Guryeva, D. Schumacher, I. Uschmann, K. S. Schulze, B. Marx, T. Kämpfer, G. G. Paulus, R. Röhlsberger, and J. Evers, Phys. Rev. Lett. **111**, 073601 (2013).
[29] R. H. Dicke, Phys. Rev. **93**, 99 (1954).
[30] Z. Ficek and R. Tanaś, Phys. Rep. **372**, 369 (2002).
[31] D.-W. Wang, Z.-H. Li, H. Zheng, and S.-Y. Zhu, Phys. Rev. A **81**, 043819 (2010).
[32] S. I. Schmid and J. Evers, Phys. Rev. A **81**, 063805 (2010).
[33] I. V. Bagratin, B. A. Grishanin, and V. N. Zadkov, Phys. Usp. **44**, 597 (2001).
[34] L. D. Landau and E. M. Lifshitz, *The Classical Theory of Fields, Volume 2 of A Course of Theoretical Physics* (Pergamon, Oxford, 1971), p. 101.
[35] L. D. Landau and E. M. Lifshitz, *Quantum Mechanics, Non-Relativistic Theory, Volume 3 of A Course of Theoretical Physics* (Pergamon, Oxford, 1965), p. 94.
[36] N. D. Scielzo, J. R. Guest, E. C. Schulte, I. Ahmad, K. Bailey, D. L. Bowers, R. J. Holt, Z.-T. Lu, T. P. O'Connor, and D. H. Potterveld, Phys. Rev. A **73**, 010501 (2006).
[37] The spontaneous decay rate of the antisymmetric subradiant entangled state is nonzero due to a finite value of the parameter kr—it is of the order of $(kr/2)^2\Gamma$. For precise evaluation, see Sec. IV model.
[38] D. D. F. Phillips, A. Fleischhauer, A. Mair, R. L. Walsworth, and M. D. Lukin, Phys. Rev. Lett. **86**, 783 (2001).
[39] There is no reason to further compare the dip effect in this paper with that in EIT: they are very different in physics, since they are controlled by different tools. Moreover, the present effect seems to be far from an experimental realization as yet, whereas EIT has been studied for more than 15 years.
[40] R. Loudon, *The Quantum Theory of Light* (Clarendon, Oxford, 1973), Chap. 8.
[41] P. R. Berman and G. W. Ford, Phys. Rev. A **82**, 023818 (2010).
[42] M. J. Piotrowicz, M. Lichtman, K. Maller, G. Li, S. Zhang, L. Isenhower, and M. Saffman, Phys. Rev. A **88**, 013420 (2013).
[43] A. Goban, C.-L. Hung, J. D. Hood, S.-P. Yu, J. A. Muniz, O. Painter, and H. J. Kimble, Phys. Rev. Lett. **115**, 063601 (2015)
[44] See Sec. 4 of Ref. [1]
[45] I. I. Sobel'man, *Introduction to the Theory of Atomic Spectra* (Pergamon, Oxford, 1972), Chap. 9.
[46] W. H. Louisell, *Quantum Statistical Properties of Radiation* (John Wiley & Sons, New York, 1973), Chap. 5.
[47] H. A. Bethe, Phys. Rev. **72**, 339 (1947).
[48] P. R. Berman and G. W. Ford, in *Advances In Atomic, Molecular, and Optical Physics*, edited by E. Arimondo, P. R. Berman, and C. C. Lin (Elsevier, Amsterdam, 2010), Vol. 59, p. 175.

[49] A. A. Makarov, V. T. Platonenko, and V. V. Tyakht, Sov. Phys. JETP **48**, 1044 (1978).
[50] A. A. Makarov, B. D. Pavlik, and O. V. Tverdokhlebova, Ukr. Fiz. Zh. **29**, 952 (1984), in Russian.
[51] A. A. Makarov, in *Laser Spectroscopy of Highly Vibrationally Excited Molecules*, edited by V. S. Letokhov (Adam Hilger, Bristol, 1989), p. 106. See Appendix 3A of this paper.
[52] V. S. Vladimirov, *Equations of Mathmatical Physics*, Pure and Applied Mathmatics Vol. 3 (Marcell Dekker, New York, 1971).
[53] See, e.g., p. 75 in Ref. [52], or the so-called Poincaré-Bertrand transformation formula [54].
[54] N. I. Muskhelishvili, *Singular Integral Equations: Boundary Problems of Function Theory and Their Application to Mathematical Physics* (Dover, New York, 1992), Chap. 23.